



# Two chironomid-inferred mean July air temperature reconstructions in the South Carpathian Mountains over the last 2000 years

The Holocene  
1–18  
© The Author(s) 2024  
Article reuse guidelines:  
sagepub.com/journals-permissions  
DOI: 10.1177/09596836241236353  
journals.sagepub.com/home/hol  
**S Sage**

Zoltán Szabó,<sup>1</sup>  Krisztina Buczkó,<sup>1,2,3</sup> János L Korponai,<sup>4,5</sup>  
Tomi Luoto,<sup>6</sup> Róbert-Csaba Begy,<sup>7,8</sup> Artitina Haliuc,<sup>1,9</sup>   
Daniel Veres,<sup>9</sup> Ladislav Hamerlík,<sup>10,11</sup> Réka Csorba,<sup>1</sup>  
Andreea Rebea Zsigmond,<sup>5</sup> Gabriella Darabos,<sup>1</sup>  
Nikoletta Méhes,<sup>12</sup> Csilla Kövér<sup>1</sup>  
and Enikő Katalin Magyari<sup>1,13</sup>

## Abstract

We present chironomid-based reconstructions of mean July air temperature changes over the last 2000 years from Lake Latoriței (1530 m a.s.l.) in the Southern Carpathians. A multi-proxy analysis was performed along a 58 cm long sediment core and two training sets were used for quantitative July air temperature reconstructions: the Eastern-European (EE, 212 lakes) and the Finnish-Polish-Carpathian (FPC, 273 lakes). The transfer functions had a coefficient of determination ( $r^2$ ) 0.88 and 0.91 with a root mean squared error of prediction (RMSEP) 0.88°C and 1.02°C. Despite possible biases resulting from methodological problems and the ecological complexity of the chironomid response to both climatic and environmental changes, the agreement of the temperature reconstruction of Lake Latoriței with other alpine records suggests that the transfer function successfully reconstructed past summer temperatures between 750 and 1830 CE. Biases in the temperature reconstruction in the period before 750 and after 1830 CE were likely caused by increased abundance of rheophilic and semi-terrestrial chironomid species related to increased inflow activity before 750 CE and local land use changes after 1830 CE, which was also indicated by increasing deforestation and increasing lake productivity in the pollen and diatom records. Our results suggest that the region experienced a warm period between 750 and 1360 CE, and a cold period between 1360 and 1600 CE followed by fluctuating summer temperatures until 1830 CE. These events were associated with the so-called 'Mediaeval Warm Period' (MWP) and the 'Little Ice Age' (LIA), respectively. The inference models reconstructed a decrease in July air temperatures by 0.7°C–1.1°C during the LIA relative to the warmer MWP. We also demonstrated that the FPC training set gives better results, supporting that local/continental training sets are efficient to detect weak amplitude summer temperature changes in the Late-Holocene.

## Keywords

chironomids, Finnish-Polish-Carpathian training set, Late-Holocene, mean July air temperature reconstruction, multi-proxy palaeoecology, RWP-LALIA-MWP-LIA

Received 27 January 2023; revised manuscript accepted 29 January 2024

<sup>1</sup>Department of Environmental and Landscape Geography, Eötvös Loránd University, Hungary

<sup>2</sup>Department of Botany, Hungarian Natural History Museum, Hungary

<sup>3</sup>Center for Natural Science, University of Pannonia, Research Group of Limnology, Egyetem, Hungary

<sup>4</sup>Department of Water Supply and Sewerage, Faculty of Water Sciences, University of Public Service, Hungary

<sup>5</sup>Department of Environmental Science, Sapientia Hungarian University of Transylvania, Romania

<sup>6</sup>Faculty of Biological and Environmental Sciences, Ecosystems and Environment Research Programme, University of Helsinki, Finland

<sup>7</sup>Faculty of Environmental Science and Engineering, 'Babes-Bolyai' University, Romania

<sup>8</sup>Interdisciplinary Research Institute on Bio-Nano-Sciences, Babes-Bolyai University, Romania

<sup>9</sup>Institute of Speleology, Romanian Academy, Romania

<sup>10</sup>Matej Bel University, Faculty of Natural Sciences, Slovakia

<sup>11</sup>Institute of Zoology, Slovak Academy of Sciences, Slovakia

<sup>12</sup>West-Transdanubian Water Directorate Department of Water Conservation and River Basin Management, Laboratory, Hungary

<sup>13</sup>HUN-REN-MTM-ELTE Research group for Paleontology, Hungary

## Corresponding authors:

Zoltán Szabó, Department of Environmental and Landscape Geography, Eötvös Loránd University, Pázmány Péter str. 1/C, Budapest H-1117, Hungary.

Email: szotyis3@caesar.elte.hu

Enikő Katalin Magyari, Department of Environmental and Landscape Geography, Eötvös Loránd University, Pázmány Péter str. 1/C, Budapest H-1117, Hungary.

Email: eniko.magyari@ttk.elte.hu

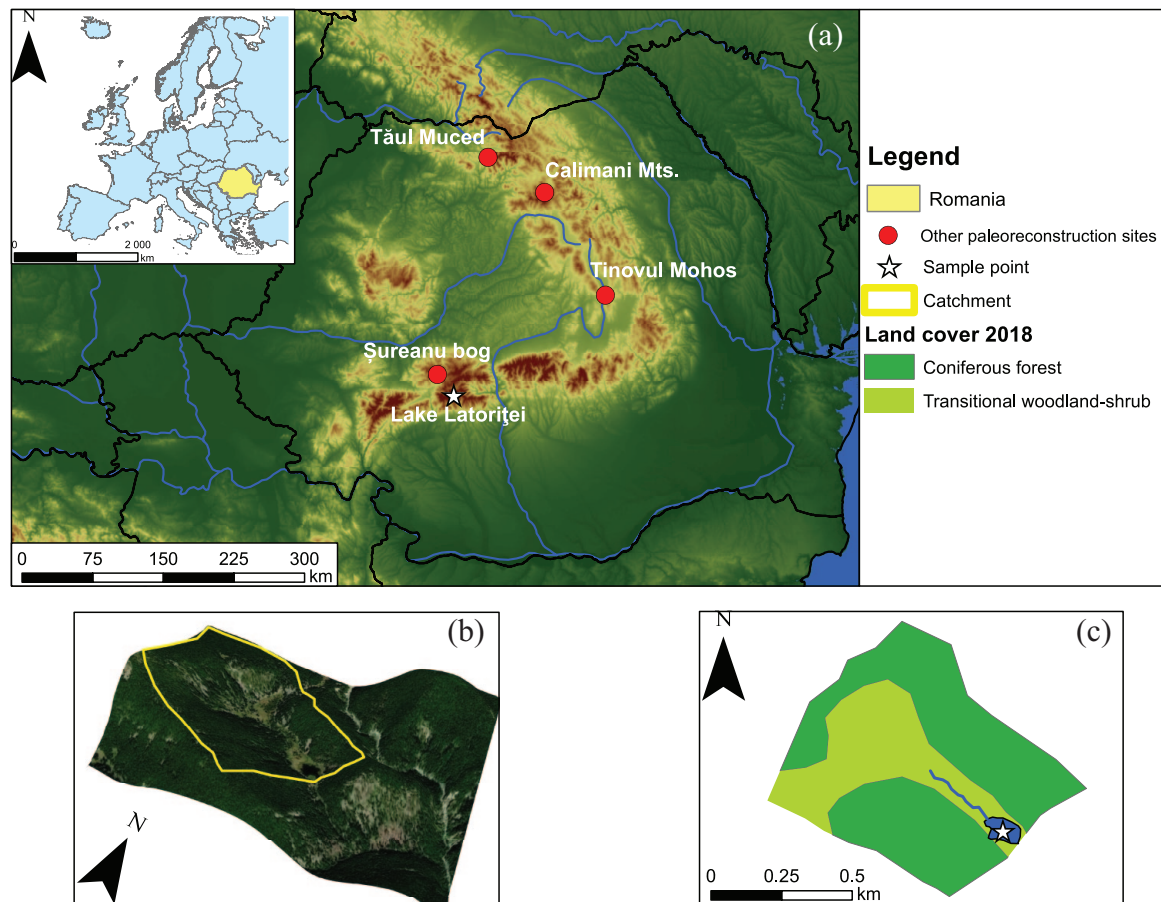


**Figure 1.** The location of the study area within Europe and Romania with some palaeohydrological (Diaconu et al., 2020; Feurdean et al., 2015; Longman et al., 2019) and palaeotemperature (Popa and Kern, 2009) reconstruction sites in Romania (a) with a digital elevation model of the Lake Latoritei catchment combined with satellite image (b); we also show a satellite image (2020) based land cover classification of the Lake Latoritei catchment with the location of the short gravity cores (c); image source: Esri, i-cubed, USDA, USGS, AEX, GeoEye, Getmapping, Aerogrid, IGN, IGP, UPR-EGP and the GIS User Community, ESRI.

## Introduction

Alpine and arctic areas are warming at an unprecedented rate relative to the rest of the planet due to a variety of climate feedback mechanisms (Axford et al., 2009; Cantonati et al., 2021; Pörtner et al., 2022; Smol, 2019). To distinguish anthropogenic from natural forced climate variation and to evaluate the performance of climate model simulations, absolutely dated climate records from these regions into the Late-Holocene are crucial. In the Carpathian Mountains lakes provide many opportunities for outdoor recreation and tourism, but growing visitor numbers and global changes (e.g. atmospheric artificial fertiliser input, heavy metal and organic pollutant input, warming water temperatures) increase negative effects on their recreational values by leading to eutrophication (Cantonati et al., 2021; Haliuc et al., 2020; Kuefner et al., 2020; Szabó et al., 2020). To understand their functioning and forecast their expected ecosystem trajectories, we need to quantify how these lakes have responded to previous warming events and what was the amplitude of warming in the past. Targeted management strategies require such knowledge. As a first step along this line, we examine in this paper how fossil chironomid assemblages record summer temperature change in the continental part of Europe. We focus on East-Central Europe (as defined by Halecki (1950, Figure 1), a region that is relatively understudied, where the South Carpathian mountain range abounds in alpine lakes with rich chironomid fauna allowing for quantitative warmest month mean temperature reconstructions (Szabó et al., 2020; Tóth et al., 2015). The approach we use builds

upon the indicative value of Chironomidae (non-biting midge) larval remains, the head-capsules of which are well preserved in lake sediments. Chironomid assemblages have been widely used to reconstruct July and summer mean temperature changes in alpine areas because of their short-life cycles and high sensitivity to temperature variations (Eggermont and Heiri, 2012; Heiri et al., 2011; Luoto, 2009; Tóth et al., 2015). Statistical analyses of both instrumental data and reconstructed temperature data confirm that chironomid communities are good summer or mean July air temperature ( $T_{July}$ ) indicators in low trophic environments in the cold temperate and boreal zones (Brooks et al., 2007; Heiri et al., 2011; Luoto et al., 2019; Self et al., 2011; Walker, 1987, 2001). Problems can naturally arise when modern analogue data sets are incomplete or the chironomid assemblages are affected by other concurrent environmental factors such as landscape, vegetation and population changes (Eggermont and Heiri, 2012; Larocque et al., 2009; Larocque and Bigler, 2004; McKeown and Potito, 2015). In addition to confounding environmental variables, such as nutrients and anoxia (Brodersen and Quinlan, 2006; Eggermont and Heiri, 2012; Medeiros et al., 2015), a potential downside of chironomids as palaeotemperature proxy lies in the suitability of the training set to the downcore site (Engels et al., 2014). In an ideal situation, the downcore site should be within the geographical area of the training set, the study site characteristics (such as lake size and depth) should be similar, and the calibration sites should constitute a temperature gradient that covers the expected range of past temperature changes. When applying inference models to cores outside the training set's geographical

or environmental range, problems related to taxon occurrences (poor modern analogues) and unrealistic taxon-specific temperature optima arise. Moreover, continental-scale calibration sets (Heiri et al., 2011) may not be able to detect small-magnitude variation in temperatures, although they can be very useful in reconstructing large-scale climate patterns (Luoto et al., 2019).

In Europe, relatively few chironomid-based temperature reconstructions were published for the last 2000-year with decadal resolution, and most of them come from high elevation sites (1700–2400 m a.s.l.) in the Alps (Bigler et al., 2006; Ilyashuk et al., 2019; Larocque-Tobler et al., 2010, 2012). Overall, these records suggest a large regional difference in the manifestation of cold summers during the Little Ice Age (LIA) along a west-east mountain gradient in Europe.

Our study site, Lake Latoriței (Lacul Iezerul Latoriței, 1530 m a.s.l.; Figure 1) is an alpine lake in the South Carpathians. In order to explore whether past and present climatic changes are detectable in the sediment record of Lake Latoriței, we analyse a 58 cm sediment core roughly covering the last 2000-year. We perform a chironomid-based mean July temperature reconstruction. In addition, multi-proxy methods (loss-on-ignition (LOI), major and trace element, cladoceran, diatom, pollen and micro-charcoal analyses) are used to disentangle climatic and anthropogenic factors. Our aims are (1) to evaluate the reliability of the chironomid-based temperature reconstructions and assess the summer climatic trend of the region; (2) to evaluate the applicability of the East European (EE) training set and its newly extended version (Finnish-Polish-Carpathian; FPC) for reconstructing Late-Holocene summer temperatures; and finally, (3) to evaluate whether temperature was the main driver of the chironomid assemblage changes during the industrial period, when human impact intensified.

## Regional setting

### *The Parâng Massif and Lake Latoriței*

Our study site is located in Munții Latoriței (45°22′01.7″N, 23°42′04.0″E) that is part of the Parâng Massif of the Southern Carpathians. The area is dominated by Proterozoic and Palaeozoic granite, gneiss, and amphibolite rocks. Pleistocene glaciers affected the region above 2000 m a.s.l. and also descended to 1300–1400 m a.s.l. (Gheorghiu et al., 2015; Pinczés, 1995; Urdea et al., 2011). Altogether, more than 15 cirques, 20 glacial niches and 12 ice aprons were formed in Munții Latoriței (Urdea et al., 2011).

In the 1970s in the Latoriței surroundings, a decrease in forest area took place due to hydrotechnical construction on main river valleys and development of tourist infrastructures (Marinescu et al., 2013). The national road, Transalpina (DN67C) is the highest road of the country and links two historical regions, Transylvania and Tara Românească. It is an old road transhumance, used by shepherds to cross the Carpathians and appears on historical maps as a Roman strategic corridor. A road accessible to cars was constructed between 1934 and 1939 and modernised after 2009.

Lake Latoriței is situated at an altitude of 1530 m a.s.l., with a catchment area of 0.57 km<sup>2</sup>, a lake surface area of 0.8 ha and a maximum depth of 1.5 m. The lake surface to watershed ratio is 1:71. Located in the upper basin of a glacial valley, the lake has been a nature reserve since 2000 CE. It is fed by an active, north-flowing stream through a peat moss and sedge cover that breaks into two branches with an outflow to the south side of the lake (Figure 1) (Gheorghiu et al., 2015). The climate of the Parâng Massif is temperate continental with westerly and south-westerly winds (Voiculescu and Török-Oance, 2000). The west-east orientation of the ridge forms a barrier between the southern, humid Mediterranean, and the colder northern air masses. The annual mean temperature above 2000 m is <0°C. Annual precipitation is

between 800 and 1200 mm in lower areas (<1500 m a.s.l.) (Gheorghiu et al., 2015; Urdea and Florin, 2000). In areas above 1500 m a.s.l., precipitation often occurs in the form of snow (>150 snow covered days), while in the lower areas the effect of the foehn winds are prevalent (Gheorghiu et al., 2015).

At the altitude of the lake, the annual mean temperature is 5.8°C, the warmest month is July (15.1°C) and the coldest is January (−4.3°C). The annual precipitation is around 1065 mm. The wettest months are May, June and July, when monthly rainfall exceeds 130 mm, while the driest month is February (41 mm) based on meteorological data from the Parâng meteorological station (average values for 2015–2021; 45°23′14.3″N, 23°27′47.0″E). According to the CARPATCLIM database (1981–2010; Spinoni et al., 2015) recalculated to 1530 m using a lapse rate 0.72°C/100 m (Micu et al., 2015), the average annual temperature is 5.4°C, July mean 14.8°C, January mean −1.9°C. The annual precipitation is around 1015 mm.

The lake was chosen for palaeoecological study because of its protected location in a well isolated valley, away from direct human activity at mid altitude. Since it is situated in the middle of the altitudinal range of the montane spruce forest zone, we expected that the terrestrial vegetation has changed little in the last 2000 years apart from possible episodic wood-cuts and grazing. Since in this vegetation belt lakes are usually oligotrophic, we expected that environmental variables other than temperature will show little change, helping the reliability of our chironomid-based  $T_{July}$  reconstruction.

## Materials and methods

### *Sediment sampling and laboratory analyses*

In July 2017, a 58 cm sediment core (LIL-surface 2017-01, N 45°22′11″, E 23°42′05″) was retrieved from the central part of Lake Latoriței using an Uwitec Gravity corer with a 100-cm long chamber and 7 cm diameter. At the core location the water depth was 1.4 m. The core was sliced into 1 cm sections in the field and stored at 4°C until further examination. <sup>210</sup>Pb/<sup>137</sup>Cs dating, <sup>14</sup>C dating, chironomid, cladoceran, diatom, pollen, microcharcoal and geochemical analyses were performed on this core.

### *Historical climate trends in the Parâng Massif*

The historical meteorological data used in the present study (temperature and precipitation) was obtained from CRU (Climate Research Unit, version 4.03), a gridded dataset with 0.5° × 0.5° spatial resolution (Harris et al., 2014). The dataset covers the interval from 1901 to 2018 CE. From the original temperature and precipitation data, monthly means and annual means were calculated (Supplemental Material 1 (SM1) Supplemental Figure 1).

### *<sup>210</sup>Pb/<sup>137</sup>Cs and <sup>14</sup>C dating*

For gamma spectrometric measurements samples were placed in sealed plastic tubes and stored for at least 28 days. Subsequently, the activity concentration of <sup>226</sup>Ra was measured using the gamma lines of the short-lived radionuclide daughters of <sup>222</sup>Rn (<sup>214</sup>Pb at 295 and 351 keV and <sup>214</sup>Bi at 609 keV). Samples were analysed with a high resolution gamma spectrometer equipped with an HPGe well-type ORTEC GEM detector, having a FWHM of 1.92 keV at 1.33 MeV able to detect low gamma energies. The activity concentrations were calculated using the relative method with IAEA 385.327 and 447 standards. In the lower layers with smaller activity concentration, the <sup>210</sup>Pb<sub>tot</sub> content of the sediment was measured by its daughter radionuclide <sup>210</sup>Po, the two elements reaching equilibrium after 2 years. The <sup>210</sup>Po content of each sediment sample was determined using an aliquot of 0.5 g dry sample. 0.3 mL 100 mBq mL<sup>−1</sup> <sup>209</sup>Po tracer was added

(having an alpha energy of 4.9 MeV) to determine chemical efficiency.

Seven samples from the deeper sediment layers were selected for AMS  $^{14}\text{C}$  dating (31–32, 34–35, 37–38, 41–42, 44–45, 47–48, 51–52 cm) (SM1 Supplemental Table 1). Dating was performed on bulk lake sediment. All  $^{14}\text{C}$  ages were calibrated into calendar years using the Calib Rev. 7.0.4. software and the IntCal20 curve (Reimer et al., 2020; Stuiver and Reimer, 1993). The age-depth model was constructed using polynomial regression (Blaauw, 2010) in the CLAM package in R.

**LOI, sediment chemistry.** Loss-on-ignition (LOI) analyses were performed on 1 cm<sup>3</sup> subsamples taken contiguously at 1 cm intervals. Samples were combusted at 550°C for 4 h (Heiri et al., 2001). For the major and trace element analyses, 0.25 g dry samples were diluted in 3 mL 65% HNO<sub>3</sub> (Merck, Suprapur) and 9 mL 36% HCl (Merck, Suprapur). Microwave digestion was applied (Speedwave Entry, Berghof, Germany). The solution was diluted to 50 mL with ultrapure water. Elemental analyses were performed in a microwave plasma atomic emission spectrometer (MP-AES Model 4210, Agilent, USA). Nitrogen plasma temperature in the analytical zone was 4500 K. The concentration of the following 21 elements was determined: Al, Ba, Ca, Cd, Co, Cr, Cu, Fe, K, Li, Mg, Mn, Mo, Na, Ni, Pb, Rb, Si, Sr, V, Zn. Sedimentary chlorophyll was analysed using spectrophotometry (Jenway 6705 UV/Visible Scanning Spectrophotometer).

#### Chironomid analysis

Dry sediment samples weighing 0.09–0.5 g were investigated at 1 cm resolution between 1 and 46 cm, and at 2 cm resolution between 46 and 58 cm. Following 10% KOH treatment, samples were sieved with a 100- $\mu\text{m}$  mesh. Chironomid larval head capsules were picked from a Bogorov-counting tray (Gannon, 1971) under a stereomicroscope at 40x magnification. Larval head capsules were mounted on microscope slides in Euparal<sup>®</sup> mounting medium for microscopic identification. Identification followed Brooks et al. (2007), Rieradevall and Brooks (2001), Wiederholm (1983) and Andersen et al. (2013). Ecological groups were formed on the basis of species types (based on habitat, trophic status, and vegetation-binding) using autoecological information available from the literature (Brooks et al., 2007; Møller Pillot, 2013; Sæther and Wang, 1996; Vallenduuk and Møller Pillot, 2007, 2009; Wiederholm, 1983). Chironomid head capsule concentration was estimated by counting all head capsules in the subsamples. At least 50 (mean: 139, min.: 45, max.: 441) head capsules were identified in each sample, except from four samples (44, 48, 52, 56 cm), where 45–48 head capsules were found.

**Cladocera analysis.** Subfossil Cladocera analysis was carried out on the chironomid samples in order to detect sediment units with and without cladoceran remains and to reveal the main trends in the Cladoceran community change. Since the chironomid samples did not contain the 38–100- $\mu\text{m}$  sediment fraction, the faunal composition is biased towards the larger body parts. However, most body part remains (headshields, carapaces) are usually bigger than 100- $\mu\text{m}$ , therefore the taxonomic composition is likely complete with this analysis. Abundances are given on a semi-quantitative scale ranging between 1 and 3. Each sample was stained with safranin. The taxonomic identification followed Szeroczyńska and Sarmaja-Korjonen (2007).

**Diatom analysis.** A total of 40 samples were analysed for diatoms; every centimetre was counted in the top 26 cm, and every second between 28 and 58 cm. The wet sediment was digested in 30% H<sub>2</sub>O<sub>2</sub> then washed several times with deionised water. The cleaned valves were dried on coverslips and embedded in Naphrax

resin (Battarbee, 1986). Diatom counting was performed with a Leica DM LB2 light microscope equipped with 100 HCX PLAN APO objectives at 1000 $\times$  magnification under oil immersion and phase contrast. A minimum of 350 valves were counted per slide. Diatom data were converted into relative abundances and plotted using the programme Psimpoll 4.27. Diatom identification was based mainly on Krammer and Lange-Bertalot (1986, 1988, 1991a, 1991b), Lange-Bertalot et al. (2017), Lange-Bertalot and Metzeltin (1996) and Reavie and Kireta (2015). Nomenclature and some taxonomic concepts were updated using AlgaeBase (Guiry and Guiry, 2023). *Staurosira venter*, *S. construens*, *S. parasitoides*, *Staurosirella oldenburgiana*, *S. pinnata*, *Pseudostaurosira brevistriata*, *P. elliptica*, *P. subconstricta* were grouped as these small-celled diatom taxa are often mentioned as representatives of benthic fragilarioids.

**Pollen analysis.** A total of 10 samples were selected for pollen analysis to examine vegetation changes during the last ~2000 years. 0.25–0.3 g dry subsamples were prepared using standard methods but excluding acetolysis (Bennett and Willis, 2001). Pollen, spores and microcharcoal (length > 10  $\mu\text{m}$ ) particles were counted and identified under an Olympus BX43 light microscope at 400 $\times$  and 1000 $\times$  magnification. At least 500 terrestrial pollen grains were counted on each slide. For pollen identification, the pollen atlases of Reille (1992, 1995, 1998) and the pollen identification key of Moore et al. (1991) were used.

#### Statistical methods and chironomid-based July mean temperature reconstruction

Chironomid, geochemical and diatom assemblage zones were determined by hierarchical cluster analysis (CONISS) in Psimpoll 4.27. The statistical significance of zone boundaries was tested by the broken stick model (Bennett, 2007).

We used rate-of-change analysis (RoC, Grimm and Jacobson, 1992) in Psimpoll to estimate compositional change per unit time in the chironomid and diatom records. To estimate RoC, datasets were first interpolated to a constant time interval of 10 years (see Szabó et al., 2020).

Due to the assumed linear relationship between our variables, we chose principal component analysis (PCA) for the geochemical and chironomid data to determine major trends in the records. Prior to PCA, chemical data were Wisconsin double transformed (transformations in two steps: standardisation of chemical components by maxima at first, then site by site total), while chironomid, pollen and diatom counts were Hellinger transformed (Legendre and Gallagher, 2001). Different data transformation methods were used because of magnitude differences in case of the chemical data, while the biotic proxies had no scale differences. In this case Hellinger transformation is ideal, as it moderately reduces the weight of dominant taxa and increases the weight of rare taxa. Redundancy data analysis (RDA) was used to explore the relationship between changes in the chironomid and diatom assemblages and other environmental variables. This analysis was chosen because the gradient length of the first axis was less than four SD units (Legendre and Legendre, 2012). RDA used the first two PCA axes of the geochemical records. To examine whether chironomid community changes show any correlation with July and summer mean temperature changes in the last 120 years, we used generalised additive models (GAM, Hastie and Tibshirani, 1990) with Gaussian distribution, mean July air temperature ( $T_{\text{July}}$ ) and mean summer air temperature (=Jun-Jul-Aug;  $T_{\text{summer}}$ ) as predictors and a fixed variance structure in the model.

We used the R software environment for our multivariate data analyses (R Core Team, 2020). All statistical analyses were performed using the vegan (Oksanen et al., 2015) and rioja (Juggins, 2017) packages.

The chironomid-inferred July air temperature reconstruction ( $T_{\text{July}}$ ) was based on weighted averaging partial least-squares regression (WA-PLS; Ter Braak and Juggins, 1993) using the merged Finnish-Polish (East-European, EE; Luoto, 2009; Luoto et al., 2019; Plóciennik et al., 2021) and the new Finnish-Polish-Carpathian (Finnish-Polish-Carpathian, FPC) chironomid-temperature training sets (SM1 Supplemental Figures 2 and 3). Since the FPC training set includes 59 additional lake surface samples from the South Carpathians, we provide statistical description of this dataset, present water chemistry and July mean temperature values for each locality in Supplemental Material 2. Taxa that did not occur in the training sets were excluded from the temperature reconstruction (see SM1 Supplemental Figure 5 – grey colour taxa). In case of the FPC training set, mean July air temperatures were calculated for the new Romanian Carpathian entries using the CARPATCLIM database (Spinoni et al., 2015; 1981–2010 period,  $0.72^{\circ}\text{C}/100\text{m}$  lapse rate). The EE training set includes surface sediment samples from 212 lakes. It covers a wide altitudinal, latitudinal, lake water pH and air temperature range (Luoto, 2009; Luoto et al., 2019; Plóciennik et al., 2021). Prior to the temperature reconstruction, the percentage chironomid data were square-root transformed.

Summer air temperature reconstructions and sample-specific errors of prediction (eSEP) based on bootstrapping (999 bootstrap cycles) were calculated using the programme C2 (Juggins, 2007). The number of useful regression calibration components was estimated using  $t$ -test ( $\alpha=0.05$ ). Model performance was evaluated using jack-knife cross-validation and subsequent coefficient of determination ( $R^2_{\text{jack}}$ ), root mean squared error of prediction (RMSEP) and mean and maximum biases (SM1 Supplemental Figure 4, SM1 Supplemental Table 4, Supplemental Material 2). Using the modern analogue technique (MAT), the cut-level of the fifth percentile of all squared-chord distances in the modern calibration data was determined. These distances were then compared to the distance between each fossil assemblage and its most similar assemblage in the modern dataset and used to define ‘no close’ analogues. We make thresholds for good modern analogues in the training set (2 percentile: very good modern analogue, 5 percentile: good modern analogue, 10 percentile: fair modern analogue, 20 percentile: poor modern analogue).

In addition, the reconstructed general local trends in temperature from the last 120-year were compared with the temperature data retrieved for the area from CRU (Harris et al., 2014).

Cold climate events documented in the chironomid-based  $T_{\text{July}}$  curve are visually compared with the chronology of solar minima events recorded in the  $\Delta^{14}\text{C}$  anomalies (Stuiver et al., 1998), according to the nomenclature of Eddy (1977).

## Results and interpretation

### Age-depth model and sedimentation rate changes

We first modelled the age-depth relationship of the 58 cm long gravity core by combining  $^{210}\text{Pb}/^{137}\text{Cs}$  and AMS  $^{14}\text{C}$  dates. Figure 2 shows the results of the CLAM polynomial regression model.

According to the  $^{210}\text{Pb}/^{137}\text{Cs}$  dating results, the upper 23 cm of the sediment column covers the interval between 1797 and 2015 CE (218 years). The upper 23 cm shows an apparent  $^{210}\text{Pb}$  decay trend, suggesting modern deposition. This is supported by the  $^{137}\text{Cs}$  results. The  $^{137}\text{Cs}$  dates match well the  $^{210}\text{Pb}$  dates below 7 cm (Figure 2a), but  $^{137}\text{Cs}$  translocation is likely in the upper 7 cm. For this upper 7 cm, however, the  $^{210}\text{Pb}$  dates are well recovered and do not indicate sediment mixing. An increase in  $^{137}\text{Cs}$  concentrations is seen at depths of 8–9 cm, which is also in good agreement with the  $^{210}\text{Pb}$  results and is indicative of the Chernobyl fallout (1986 CE).

The average sedimentation rate over the past 218 years was  $0.15\text{ cm yr}^{-1}$  (Figure 2c). The accumulation rate decreases

between 13 and 23 cm (1950–1800 CE,  $<0.1\text{ cm yr}^{-1}$ ). Between 2 and 12 cm, the sedimentation rate increases significantly to  $0.24\text{ cm yr}^{-1}$ , reaching  $0.3\text{ cm yr}^{-1}$  in the upper 8 cm.

The seven AMS  $^{14}\text{C}$  dates for the interval 23–58 cm were combined with the  $^{210}\text{Pb}/^{137}\text{Cs}$  depth-age model derived ages using polynomial regression. The model suggests that the bottom of the core dates to  $\sim 190\text{ BCE}$  (Figure 2c).

### Chironomid and macroinvertebrate inferred environmental changes

Altogether 72 taxa and five statistically significant chironomid zones were identified in the sediment sequence (SM1 Supplemental Figure 5). The relative abundance diagram is presented in Figure 3, while ecological groups using habitat preference, trophic state and aquatic plant density are plotted in Figure 4.

The first zone L-1 (58–41 cm, 190 BCE–810 CE) shows high abundance of profundal taxa (51–16%; e.g. *Procladius*, *Micropsectra insignilobus*-type), terrestrial, semi-terrestrial taxa (e.g. *Mittia-Parasmittia*, *Pseudosmittia*, *Limnophyes-Paralimnophyes*) and rheophilic taxa (*Rheocricotopus effusus*-type and *R. fuscipes*-type). This taxonomic composition suggests relatively unstable water column without significant submerged vegetation. The relatively high frequency of terrestrial and rheophilic taxa (e.g. *Limnophyes-Paralimnophyes* 4–22%; *Rheocricotopus effusus*-type and *R. fuscipes*-type 2–9%) and one littoral taxon (*Heterotrissocladius marcidus*-type) indicate recurrent erosion events (stream activity), intensive flowing water and fluctuating water-level (Brooks et al., 2007; Gandouin et al., 2006; Hamerlik and Bitušik, 2009; Zheng et al., 2020). The deepest part of the lake was dominated by *Procladius* (15–37%). On the basis of the chironomid assemblage, the lake was likely mesotrophic (e.g. Bitušik and Kubovčik, 1999; Brodersen and Anderson, 2002; Brooks et al., 2007; Heiri et al., 2011; Velle et al., 2005). In addition to chironomids, we also recorded the abundance of Cladocera, Sialidae (head capsule fragments, mandibles), Trichoptera (head capsule fragments, mandibles) and Plecoptera (mandibles) remains (Figure 4). Cladocerans were important indicators of phytoplankton availability, while Sialidae, Trichoptera and Plecoptera showed riverine activity, even though many species of Trichoptera and Plecoptera also live in lakes (Newell and Baumann, 2013; Solem and Birks, 2000; Vondrák et al., 2019). The dominant cladoceran species in this zone was *Alona quadrangularis*, while *Chydorus sphaericus*, *Alona affinis* and *Graptoleberis testudinaria* were found in much smaller numbers. These cladocerans are ubiquitous due to their wide tolerance spectra. *Alona affinis* frequently occurs together with its congener *Alona quadrangularis* in the littoral zone. Although all these cladocerans are littoral species, *A. quadrangularis* is less associated with vegetation, and likes mud (Bledzki and Rybak, 2016; Sebestyén, 1965; Tremel et al., 2000). The high relative frequencies of these species suggest that lake productivity was moderate, furthermore the occurrence of the phytophile *G. testudinaria* suggests the presence of aquatic vegetation (Bledzki and Rybak, 2016). In this zone abundant Sialidae remains together with the presence of Trichoptera and Plecoptera suggest periodically intensive flowing water (Luoto et al., 2013), and overall point to strong stream activity that is in accordance with the chironomid-inferred deeper lake phase. However, the remains of Trichoptera and Plecoptera may not only indicate flowing water, as some species also live in lakes (Newell and Baumann, 2013; Solem and Birks, 2000; Vondrák et al., 2019).

The second zone L-2 (41–27.5 cm, 810–1570 CE) was dominated by littoral taxa (50–62%; e.g. *Tanytarsus mendax*-type, *Polypedium nubeculosum*-type, *Paratanytarsus penicillatus*-type) that point to a much shallower environment than in zone L-1 and a more stable water-level (Brooks et al., 2007;

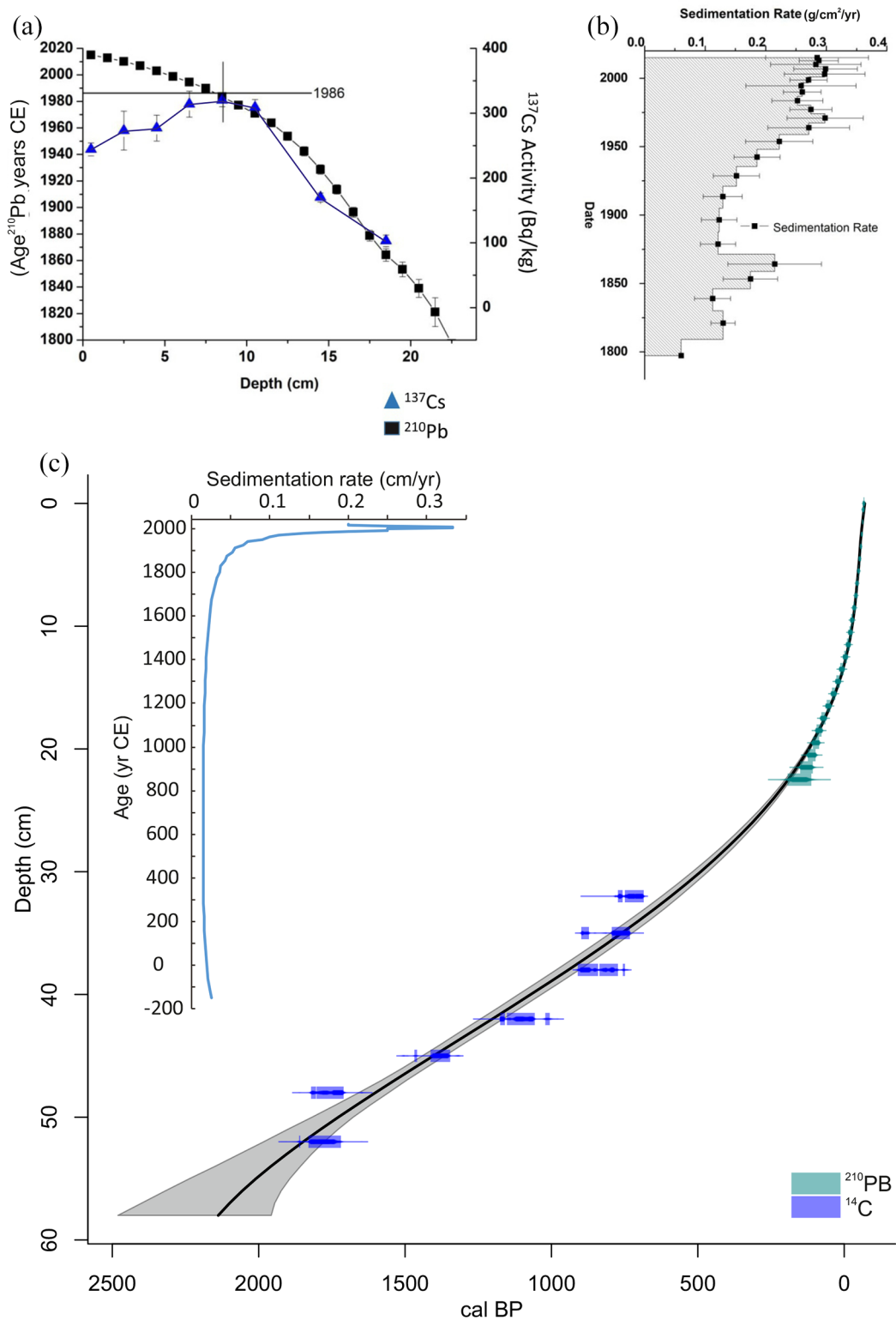


**Figure 2.** Age-depth model (a) and sedimentation rate (b) ( $\text{gcm}^{-2}\text{yr}^{-1}$ ) based on  $^{210}\text{Pb}$  and  $^{137}\text{Cs}$  measurements from Lake Latoriței gravity core; long age-depth model with sediment accumulation rates (c) based on 23  $^{210}\text{Pb}/^{137}\text{Cs}$  and 7  $^{14}\text{C}$  dates calibrated using CALIB Rev. 7.0.4. and the IntCal20 dataset; the long age-depth model (c) was constructed using polynomial regression (Blaauw, 2010) in the CLAM package in R.

Engels et al., 2008; Zheng et al., 2020). The abundance of taxa representative of the profundal (13–20%) and terrestrial zones (1–7%) decreased significantly supporting shallower lake environments. At the border of the first two zones chironomid concentration (550–1030 head capsules  $\text{g}^{-1}$ ) and taxonomic richness (29–23) increased significantly. The chironomid fauna indicate no change in the trophic state of the lake (Figure 3). At the onset of this zone Sialidae remains disappear together with a decrease in Trichoptera and Plecoptera remains (Figure 3)

suggesting a rapid decrease in stream flow at  $\sim 810$  CE (note dating uncertainty). At the same time, Cladocera remains appeared in the sediment in higher abundance with *Alona quadrangularis*, and occasionally *Chydorus sphaericus*, suggesting increased productivity. Although *Chydorus sphaericus* is considered a littoral cladoceran, it is also a member of the planktonic community in oligo- and eutrophic environments (Hořická et al., 2006; Stuchlík et al., 2017; Vijverberg and Boersma, 1997).

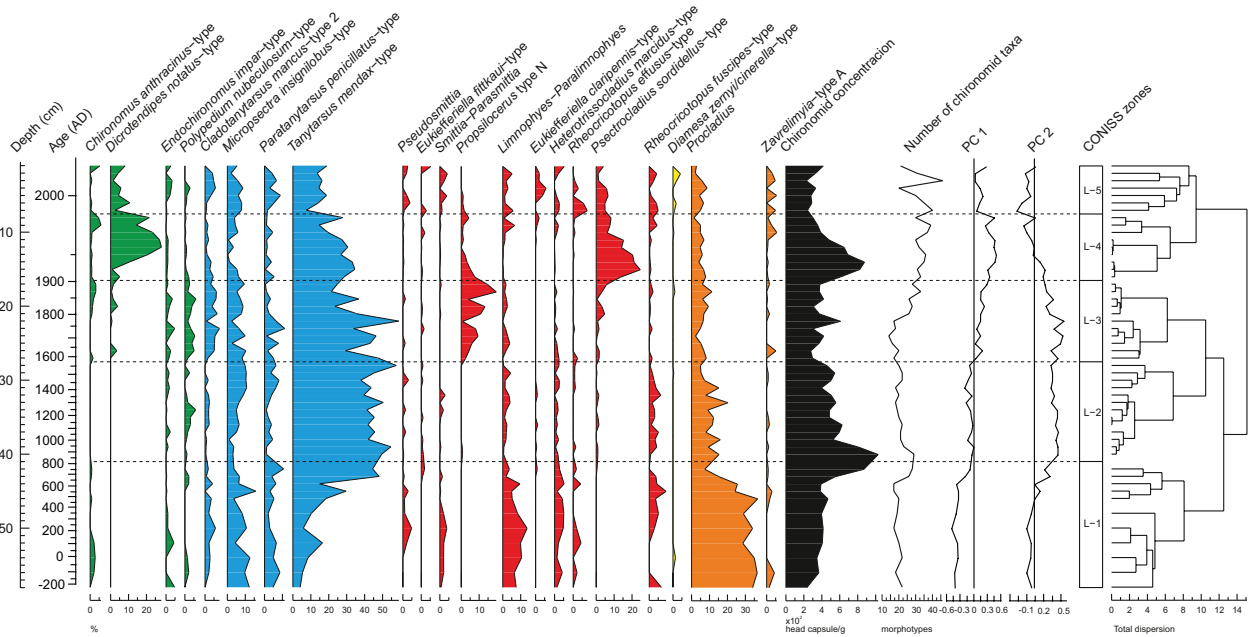


**Figure 3.** Relative frequencies of the most common chironomid taxa (>2%), values of the taxonomic richness and PC1 & 2 stratigraphic plots from Lake Latorței gravity core, Parâng Mts, South Carpathians; taxa were coloured according to subfamilies/tribes (blue: Tanytarsini, green: Chironomini, red: Orthoclaadiinae, yellow: Diamasinae, orange: Tanypodinae); significant chironomid assemblage zones (L-) were defined by CONISS.

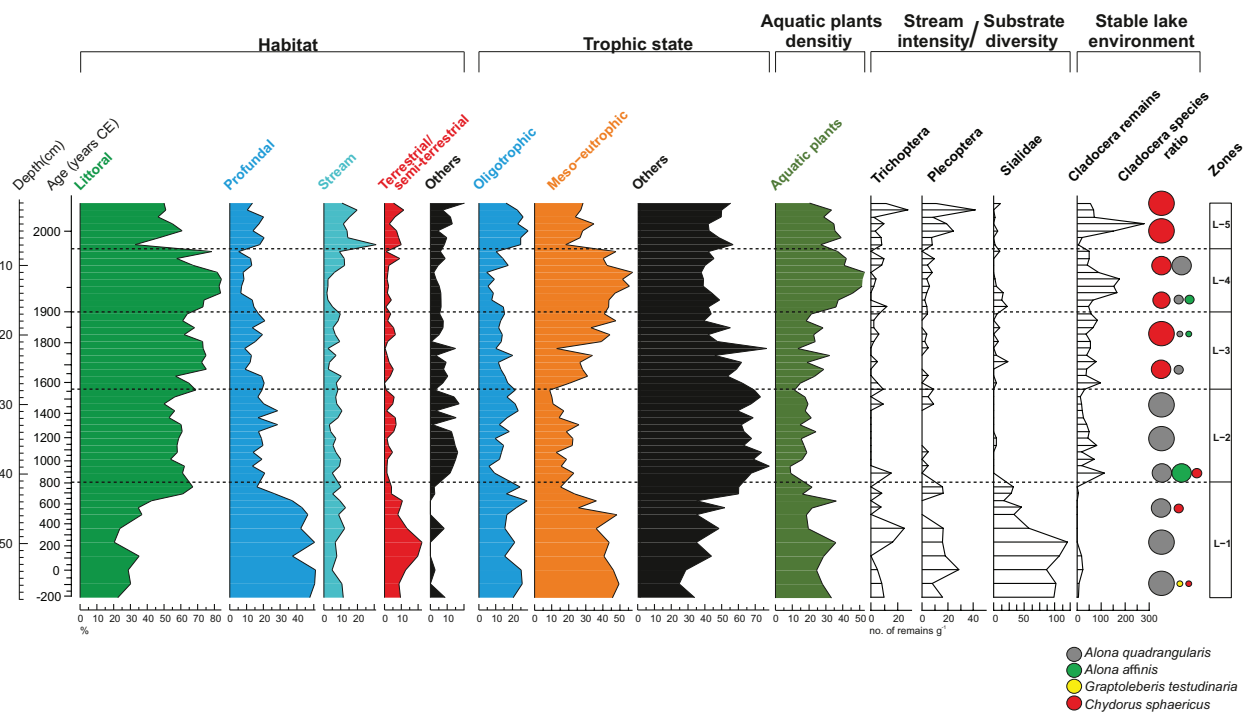


**Figure 4.** Ecological groups of the chironomid fauna on the basis of habitat preference, trophic status and vegetation-relatedness. The concentration of other macroinvertebrate groups (Trichoptera, Plecoptera, Cladocera, Sialidae) are also plotted on the right. Chironomid taxa associated with the different ecological groups are listed in SM1 Supplemental Table 3. Cladocera species abundances are relative estimates (smaller circles: rare relative abundance, bigger circles: rich relative abundance).

The third zone L-3 (27.5–16.5 cm, 1570–1900 CE) was also dominated by littoral taxa (57–75%; e.g. *Endochironomus impar*-type, *Polypedium nubeculosum*-type, *Cladotanytarsus mancus*-type 2, *Paratanytarsus penicillatus*-type, *Tanytarsus mendax*-type, *Prosilocerus* type N) indicating shallow and stable lake environment (Brodersen and Quinlan, 2006; Brooks et al., 2007; Engels et al., 2008; Gandouin et al., 2006; Zheng et al., 2020). In this zone, *Prosilocerus* type N (1–20%), *Polypedium nubeculosum*-type (1–11%) and *Cladotanytarsus mancus*-type 2 (1–8%)

appeared in higher abundance that is characteristic for more productive waters. Their increased relative abundance suggests increasing trophic level, meso-eutrophic environment (Figure 4) (Langdon et al., 2006; Sæther and Wang, 1996; Vallenduuk and Moller Pillot, 2009). Increased relative abundance of *Paratanytarsus penicillatus*-type (1–11%) and *Endochironomus impar*-type (1–5%) suggests the presence of macrophytes (Brodersen and Quinlan, 2006; Brooks et al., 2007; Zheng et al., 2020). From 1800 CE (21 cm), taxonomic richness suddenly increased (26–36

morphotypes). Increased trophic level is also indicated here by the increased concentration of cladoceran remains (Korponai et al., 2011) and the higher abundance of *Chydorus sphaericus* (Keller et al., 2002; Vijverberg and Boersma, 1997), even though this species has wide ecological tolerance. In Carpathian lakes, it was found both in ultraoligotrophic and hypertrophic lakes (Hořická et al., 2006; Sacherová et al., 2006; Stuchlík et al., 2017). Recurrent, but likely less intensive streamflow is furthermore suggested by the reappearance of Sialidae in this zone.

The fourth zone L-4 (16.5–7.5 cm, 1900–1990 CE) was characterised by the highest abundance of littoral taxa (57–84%; e.g. *Dicrotendipes notatus*-type, *Tanytarsus mendax*-type, *Psectrocladius sordidellus*-type). Profundal taxa reached minimum (6–17%), while at the end of the zone (from 1970 CE) stream (12%; e.g. *Zavrelimyia* type A) and semi-terrestrial taxa increased (2–9%; e.g. *Limnophyes-Paralimnophyes*). *Psectrocladius sordidellus*-type was present with the highest abundance (6–25%) in this zone. Since this taxon is associated with aquatic vegetation, we infer the expansion of submerged and floating macrophytes (Brooks et al., 2007; Luoto, 2010). From 1930 CE the appearance of *Dicrotendipes notatus*-type (11–28%) likely indicates an increase in air temperature and in lake productivity, and a further increase in aquatic vegetation (Brooks et al., 2007; Giaime et al., 2019; Heiri et al., 2011; Michailova, 2009). In general, chironomids in this zone indicate a shallow lake rich in aquatic vegetation, as well as increasing temperatures and/or productivity. Chironomid concentration (352–855 head capsule  $g^{-1}$ ) and taxon richness was very high. The high concentration of Sialidae remains at the onset of this zone, between 1900 and 1950 CE, is associated with increasing Plecoptera and Trichoptera concentrations, overall suggesting intensifying streamflow that halted after 1950 CE. On the other hand, this zone is characterised by the highest concentration of cladoceran remains between 1930 and 1970 CE that is in accordance with the planktonic diatom and chironomid-inferred increasing nutrient availability and consequent phytoplankton blooms (see below). Among the Cladocera species *Chydorus sphaericus* dominates, but *Alona quadrangularis* is also present in higher abundance than in the previous zone indicating high trophic level with extended littoral.

In the fifth zone L-5 (7.5–1 cm, 1990–2015 CE) the proportion of littoral taxa decreased (60–32%; e.g. *Dicrotendipes notatus*-type, *Cladotanytarsus mancus*-type 2, *Paratanytarsus penicillatus*-type, *Tanytarsus mendax*-type, *Psectrocladius sordidellus*-type), while the proportion of profundal (10–20%; *Procladius*, *Micropsectra insignolobus*-type), stream (10–31%; e.g. *Diamesa zernyi/cinerella*-type, *Eukiefferiella claripennis*-type, *E. fittkaui*-type, *Rheocricotopus effusus*-type, *R. fuscipes*-type, *Zavrelimyia* type A) and semi-terrestrial (3–11%; e.g. *Smittia-Parasmittia*, *Pseudosmittia*, *Limnophyes-Paralimnophyes*) taxa increased. The proportion of species types associated with aquatic vegetation (20–37%; e.g. *Dicrotendipes notatus*-type, *Cladotanytarsus mancus*-type 2, *Paratanytarsus penicillatus*-type, *Psectrocladius sordidellus*-type) was still high, but showed a decreasing trend. These changes suggest that erosion increased in the catchment, and the macrophyte vegetation decreased to some extent. Accelerated riverine input and the decrease in littoral taxa, together with an increase in profundal taxa suggest a modest increase in lake level in the last 20 years (Brodersen and Quinlan, 2006; Brooks et al., 2007; Gandouin et al., 2006; Luoto et al., 2011; Taylor et al., 2013). The chironomid fauna suggests that the trophic status of the lake likely decreased; it became oligo-mesotrophic. Chironomid concentration was lower (415–227 head capsule  $g^{-1}$ ) than in the previous zone, while the taxon richness was high (20–46 morphotypes). Other macroinvertebrate components of the sediment support these inferences, particularly the strong stream-flow at the onset of this zone (1990 CE). In this zone,

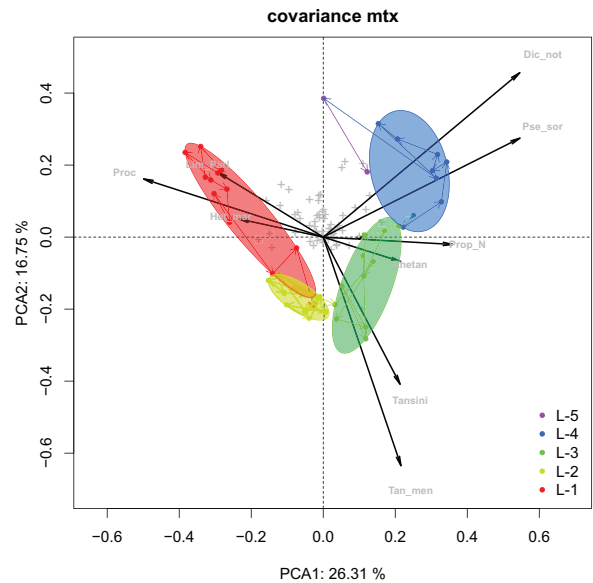


**Figure 5.** PCA of the chironomid relative frequency dataset from Lake Latorței, Parâng Mts, South Carpathians; significant chironomid zones (L-) as defined by CONISS (L-1 (190 BCE–810 CE), L-2 (810–1570 CE), L-3 (1570–1900 CE), L-4 (1900–1990 CE), L-5 (1990–2015 CE)) are marked by different colours; PCA was made on a covariance matrix using Hellinger transformation; taxa displayed had taxon scores  $>0.16$  and  $<-0.18$ ; abbreviations: Lim\_ParI: *Limnophyes-Paralimnophyes*; Proc: *Procladius*; Het\_mar: *Heterotrissocladius marcidus*-type; Dic\_not: *Dicrotendipes notatus*-type; Pse\_sor: *Psectrocladius sordidellus*-type; Prop\_N: *Propsilocerus* type N; Rhetan: *Rheotanytarsus*-type; Tansini: *Tanytarsini* indet.; Tan\_men: *Tanytarsus mendax*-type.

only *Chydorus sphaericus* is present among the cladocerans, which is eurytopic. Presence of only one Cladocera taxon likely indicates extreme conditions (e.g. low water residence time, low pH).

PCA was used to reveal major trends in chironomid community change. The first two axes explain 43% of the total variance (PC1: 26%, PC2: 17%) (Figure 5).

Along the first PC axis, negative values are associated with *Heterotrissocladius marcidus*-type, *Procladius* and *Limnophyes-Paralimnophyes*. These species occur in the bottom part of the record (L-1) in higher abundance, and we interpret negative values along PC-1 as reflecting deeper, mesotrophic lake water conditions, as well as accelerated stream-driven erosion. Positive values are associated with *Tanytarsus mendax*-type, *Tanytarsini* indet. and *Rheotanytarsus* that are indicative of an increase in the proportion of the shallow water habitats, a decrease in water-depth and erosion, and generally stable lentic conditions. PC1 thus reflects changes in water-depth (shallower with positive scores) and habitat types (extending littoral zone with positive scores). Furthermore, the association of *Propsilocerus* type N with positive sample scores suggests increasing trophic level (Brooks et al., 2007; Moller Pillot, 2013; Sæther and Wang, 1996; Wiederholm, 1983) with positive PC1 scores. The linkage of *Dicrotendipes notatus*-type and *Psectrocladius sordidellus*-type with positive sample scores also corroborates that positive values along PC1 refer to shallow lake conditions and increasing macrophyte cover. Along the PC 2 axis, positive values were associated with positive taxon loadings of *Procladius*, *Heterotrissocladius marcidus*-type, *Dicrotendipes notatus*-type, *Psectrocladius sordidellus*-type indicating mainly lacustrine conditions rich in macrophytes (probably impacted by the river), likely during more frequent floods, while negative values were shown by, *Tanytarsus mendax*-type indicating that



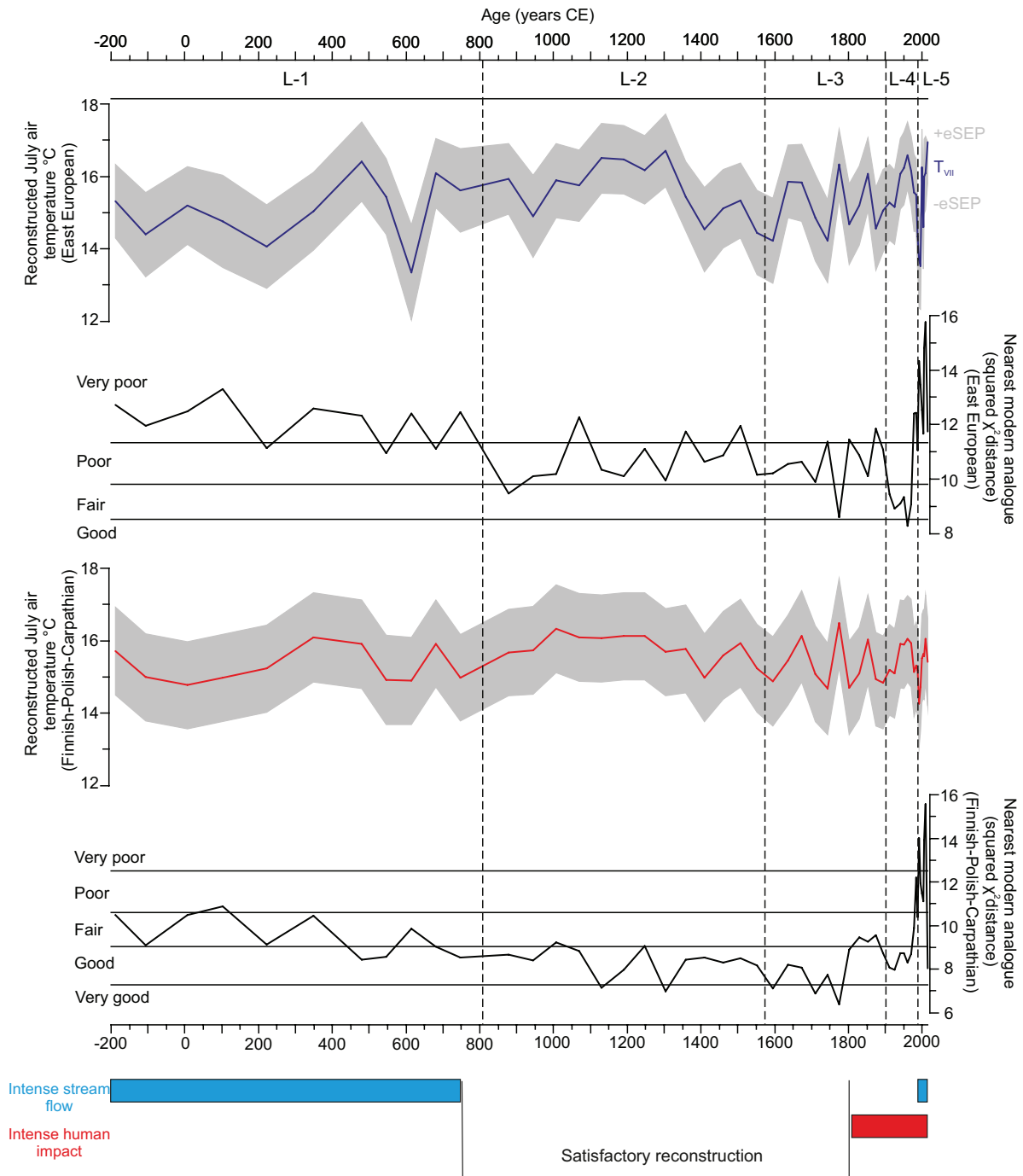


**Figure 6.** Chironomid-inferred mean July air temperatures for the last ~2000-year at Lake Latoriței, Parâng Mts, South Carpathians; the blue curve displays the WA-PLS transfer function based results using the East European (EE) training set, while the red curve is based on the Finnish-Polish-Carpathian (FPC) training set.

samples associated with negative PC2 scores were the most isolated from the river. Therefore the second axis is interpreted as reflecting changes in inflow energy/intensity.

### Summer temperature reconstruction

The reconstructed July air temperature in the last 2000-year ( $T_{July}$ ) ranged from 13.4°C to 16.9°C and showed an RMSEP value of 0.88°C when we used the Eastern European (EE) training set (Figure 6; Luoto et al., 2019). The Finnish-Polish-Carpathian training set (FPC) provided reconstructed  $T_{July}$  values between 14.3°C and 16.5°C and showed an RMSEP of 1.02°C (SM1 Supplemental Table 4). FPC extends the EE training set to the Romanian Carpathians, and includes surface sediment samples from 273 lakes (Luoto et al., 2019; Supplemental Material 2).

The reference period was 1980–2010 CE (CarpatClim data were converted to the altitude of the lake). The average July temperature value obtained for this period is 14.8°C. Both training sets overestimate the reference period temperature in the area by ~1°C. The EE chironomid-based temperature reconstruction had very poor or poor modern analogues as inferred by MAT in all fossil samples (Figure 6), while the FPC dataset had very good and good, and fair analogues suggesting that the reconstructed values are likely more reliable. For the latter, poor and very poor analogues were present only in the last 35 years.

Both temperature reconstructions show relatively cool summers with a colder period between 190 BCE and 220 CE (Figure 6). This was followed by a warmer period between 220 and 550 CE. July mean temperatures decreased again between 550 and 615 CE by ~0.5°C (FPC) and ~0.7°C (EE) (Figure 6). This was followed by

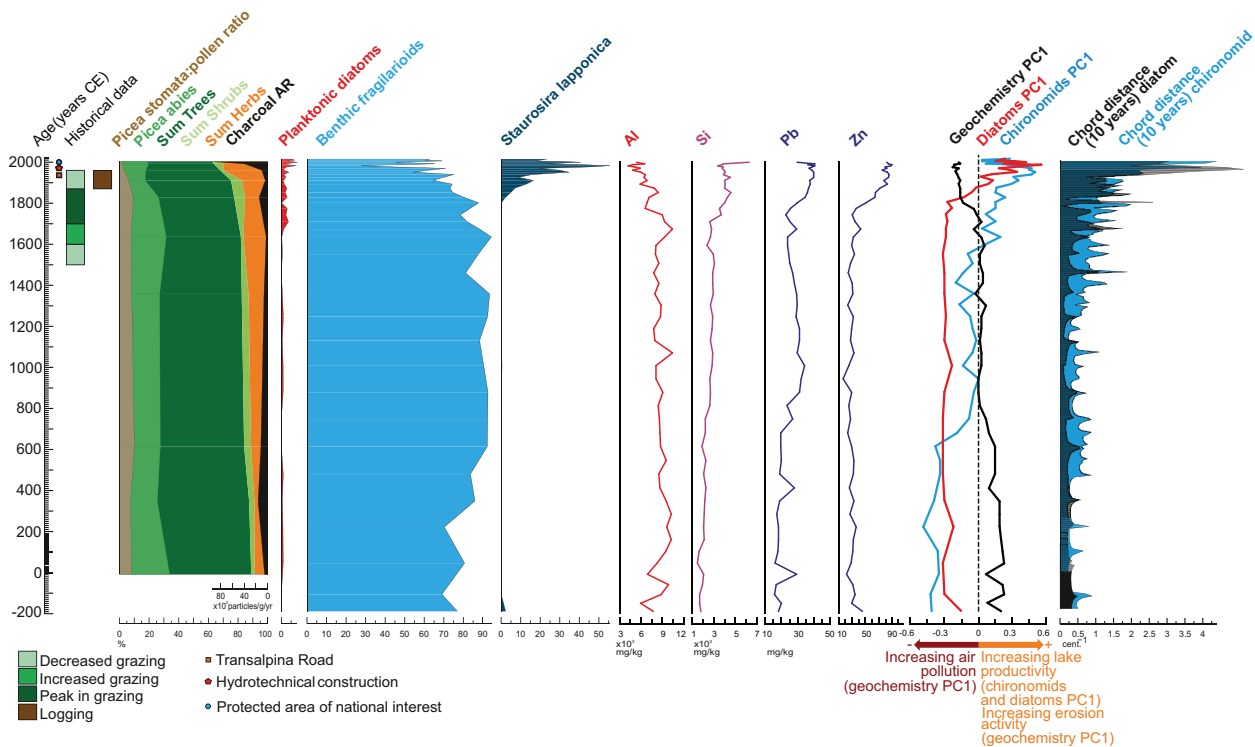


**Figure 7.** Summary on the land use, terrestrial vegetation, aquatic floristic, faunistic and lake chemistry changes as indicated by the stratigraphic PC plots and rate-of change (RoC) records for the last ~2000 years from Lake Latoriței, Parâng Mts, South Carpathians.

rapid warming at the beginning of the seventh century. The reconstructed July mean temperatures increased to 15.9°C and 16.1°C (Figure 6). Average July temperatures were around 15°C until 1300 CE. Furthermore, a generally colder period was reconstructed with both training sets between 1300 and 1895 CE. Average July temperatures were around 15.1°C–15.4°C, that is, 0.7–1.1°C colder than in the warmer period before (615–1300 CE). This was followed by rapid warming between 1895 and 1970 CE, when reconstructed July mean temperatures increased to 15.7°C–15.9°C. Both reconstructions suggest a significant temperature decrease between 1970 and 2000 CE (14.5°C–14.9°C). The amplitude of this decrease is 1°C–1.2°C (Figure 6). Finally, the warming trend after 2000 CE is present in both reconstructions (15.6°C–16°C). 1.1°C increase is reconstructed in the last 15 years compared to the 1970–2000 CE colder period (Figure 6).

When the meteorological data from CRU are compared with the chironomid-inferred July mean temperatures for the period 1901–2018 CE, the correlation coefficients are very low (0.03 with the EE and 0.11 with the FPC reconstruction), even though the trend in the measured and reconstructed temperature curves are comparable with some time lags (SM1 Supplemental Figure 6). Cross-correlation analysis also confirms that chironomid-inferred July mean temperatures show some correlation with the CRU observed July temperatures at ~15-year time lag. This suggests that (i) age estimates of the  $^{210}\text{Pb}/^{137}\text{Cs}$  depth-age model have relatively large uncertainties ( $\pm 5$  years) and the obtained ages are possibly shifted by ~10 years, and (ii) the reconstructed trophic level increase and shallowing of the lake in the last century likely had a stronger effect on the chironomid community change than summer temperature alone. We will discuss these factors further below taking into account the results of the multi-proxy analyses.

Detailed description of sediment chemistry, diatom and pollen analyses is given in Supplemental Material 1. Here we summarise the most important results of these proxies that we use for identifying periods with increased human impact and accelerated nutrient input (both atmospheric and local grazing induced) in the lake.

The chemical element data (SM1 Supplemental Figure 7, Figure 7) showed increased Al, K, F, Mg concentrations in the

bottom part of the sequence, between 190 BCE – 380 CE (58–47.5 cm) that suggested increased terrigenous input from the slopes or from the inflowing stream. This was followed by a period of decreasing clastic material input until 1975 CE, when a second increase was detected. Increasing air pollution, likely from fossil fuel combustion and vehicle emissions, was inferred from the increased concentration of heavy metals (Pb, Cu, Zn) since 1750 CE. Si closely followed the trend of trace metals indicating its possible absorption on metallic hydroxide particles (Figure 7).

The diatom record was characterised by diverse benthic diatom assemblages in the first diatom assemblage zone (DAZ-1, 58–44.5 cm, 190 BCE–580 CE) and the lack of planktonic diatoms suggested clear lake conditions with macrophytes (Figure 7, SM1 Supplemental Figure 9). From 580 CE benthic fragiliarioids were even more abundant. Since these taxa dominate in alpine and arctic lakes with a short growing season and long periods of ice cover (Lotter and Bigler, 2000), their increase suggested longer ice cover from 580 to 1830 CE (DAZ-2, 44.5–20 cm). From 1830 CE the gradual increase of *Staurosira lapponica* with heavily silicified frustules correlated with the increase in biogenic Si in the sediment (Figure 7, SM1 Supplemental Figure 9). Since Si increased along with heavy metals (Pb, Ba, Zn), we interpreted this change to be indicative of increased absorption and bioavailability of Si on heavy metal complexes. In addition, we found a permanent presence of planktonic fragiliarioids pointing to slight planktonic eutrophication. The RoC curve displayed rapidly increasing and constantly high values since 1930 CE signalling rapid and sequential reorganisation of the diatom communities (Figure 7).

The pollen record was dominated by trees with 90% arboreal pollen in the bottom of the sequence that reduced to 70% by the top (SM1 Supplemental Figure 11; Figure 7). Locally Norway spruce (*Picea abies*) was dominant. Four forest clearance episodes were detected: at ~480, ~1745, ~1940 and ~1980 CE (Figure 7 & Supplemental Figure 11). Norway spruce pollen frequencies started to decrease steadily from 1830 CE. The largest spruce forest loss was found between ~1940 and ~1980 CE. The pollen

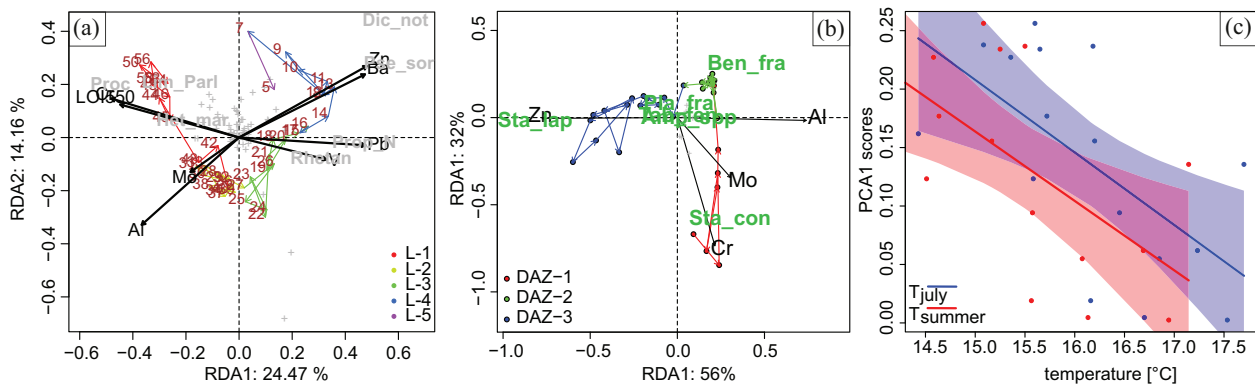


**Figure 8.** Results of the redundancy analysis (RDA); (a) significant geochemical variables (LOI, Cr, Al, Zn, Ba, Pb, V) and chironomids (Abbreviations: Lim\_Parl: *Limnophyes-Paralimnophyes*; Proc: *Procladius*; Het\_mar: *Heterotrissocladius marcidus*-type; Dic\_not: *Dicotendipes notatus*-type; Pse\_sor: *Psectrocladius sordidellus*-type; Prop\_N: *Propsilocerus* type N; Rhetan: *Rheotanytarsus*-type; Tansini: *Tanytarsini*; Tan\_men: *Tanytarsus mendax*-type); (b) significant geochemical variables and diatoms (Abbreviations: Beb\_fra: Benthic fragilarioids; Sta\_lap: *Staurosirella lapponica*; Sta\_con: *Staurosira construens*; Pla\_fra: Planktonic fragilarioids; Tab\_fen: *Tabellaria fenestrata*; Amp\_spp: *Amphora* spp); (c) General additive models (GAMs) to examine the relationship between PC I scores (chironomid taxa) and temperatures ( $T_{\text{july}}$  (blue) and  $T_{\text{summer}}$  (red)).

record suggested intensified land use since ~1745 CE with the onset of a gradual increase in anthropogenic indicator herbs (*Canabis*-type, *Plantago major/media*, *Artemisia*).

## Discussion

### Lake water quality and land use changes during the last 2000-year, possible biases of the temperature reconstructions

One aim in this study was to examine the warmest month mean temperature changes over the last 2000-year in the South Carpathian region. Since this period is characterised by human population increase, and more intensive exploitation of the alpine zone in the Carpathians and Alps (Brisset et al., 2017; Feurdean et al., 2016, 2017; Haliuc et al., 2017; Hubay et al., 2018; Vincze et al., 2017), in this section we examine if changes in other environmental factors can be detected by other proxies that might have played a role in the chironomid community changes.

Figure 7 summarises inferences drawn from the pollen, geochemical and diatom records in connection with the past 2000-year intensity of land use regionally and locally, while Figure 8 displays the result of the multivariate data analyses (for detailed results see the Supplemental Material 1).

Our multi-proxy environmental reconstruction suggested intensive stream flow, erosional activity, organic-rich detrital input between ~180 BCE and ~810 CE that encompass the Roman Warm Period (RWP), LALIA and early MWP (Figure 7). The pollen record in this period pointed to a forested landscape with spruce dominance and only a single episodic, small scale forest clearance at ~480 CE (Supplemental Figure 11). The diatom record in the same period was characterised by a diverse benthic assemblage that changed at ~580 CE, within the LALIA to a much more species poor, cold-tolerant community dominated by benthic fragilarioids (Figure 7). Trophic level increase likely in connection with forest clearance and grazing around the lake was indicated by the diatom community since ~1830 CE when biogenic silica content also increased considerably. We interpreted these changes by the absorption of Si on heavy metal pollutants that also increased since ~1830 CE. We also found the expansion of benthic fragilarioids, *Staurosira lapponica* and some nutrient indicator taxa, like *Nitzschia* and *Tabellaria fenestrata*. Both the RoC curve and PC1 values displayed a rapidly increasing and constantly high rate of change in the diatom community since ~1930 CE when the pollen record indicated the most intensive forest clearance and grazing around the lake (Figure 7). Overall, the multi-proxy analysis suggests that human impact accelerated

around the lake since 1830 CE, and from this point the chironomid faunal composition was probably also affected by land use.

### Driving factors of the chironomid assemblage changes

We have demonstrated above that human impact and land use changes intensified around Lake Latoriței in the 19th century. Similar results were also obtained from alpine lake sediment studies in the Alps and Carpathians (e.g. Hamerlík et al., 2016; Luoto and Nevalainen, 2012; Tóth et al., 2018). Ecological research in lowland lakes, on the other hand, also demonstrated that even though forest compositional and agricultural changes can be regarded as major factors influencing chironomid composition, chironomid-inferred temperature reconstructions can be still satisfactory. They correlate well with instrumental temperature records, if human impact has been stable over the investigated interval (Potito et al., 2014). As changes in the Latoriței chironomid record were concurrent not only with climate fluctuations, but also with changes in the local land use, we made statistical analyses to examine which environmental variables, in addition to temperature, might have influenced changes in the chironomid community. Using redundancy-analysis (RDA) and general additive modelling (GAM), we examined these possible relationships between sediment chemistry and the biotic proxies (Figure 8).

Overall, we found that changes in the chemical environment had a much stronger effect on the diatom community (RDA 1 & 2 explained 88% of the total variance) than on the chironomid fauna (RDA 1 & 2 explained 39% of the total variance; Figure 8). RDA also shows that Zn, Ba, Pb, V, Al, Mo, Cr, LOI along the first (24.47%) and Zn, Ba, Al along the second RD axis (14.16%) co-varied with the chironomid community. Since high Al, Cr concentrations and high LOI values characterised periods with stronger stream activity, their covariance with *Procladius* and *Limnophyes-Paralimnophyes* suggests weak affinity of this community to both inorganic and organic stream-driven terrigenous material input (Hamerlík et al., 2016; Zheng et al., 2020; Wilson and Gajewski, 2004), which means that the representation of these taxa has been affected by inflow activity to a small extent. Furthermore, the covariance of Zn, Ba, Pb (heavy metals) with *Psectrocladius sordidellus*-type and *Dicotendipes notatus*-type suggests a possible indirect connection between atmospheric pollution and chironomid community change. The concentration of these elements increased in zone G-3 (~1760–2000 CE; SM1 Supplemental Figure 7) and coincided with a warmer, more productive, and aquatic macrophyte-rich lake

environment (Tóth et al., 2019; Vallenduuk and Moller Pillot, 2009), but the temperature tolerances of the responding chironomid taxa vary quite widely (Brooks et al., 2007; Heiri et al., 2011; Luoto et al., 2019). Given the overall weak explanatory power of RDA axes 1 & 2 in case of the chironomid fauna (Figure 8), we conclude that the prevalence of atmospheric heavy metal pollution since ~1750 CE (intensified after 1830 CE) likely explains some of the chironomid community compositional change indirectly (e.g. caused by the coincident macrophyte expansion in the lake). Nonetheless, other environmental factors, such as warmest month temperature fluctuations, need to be invoked to explain the rest of the variance.

In order to examine the dependence of the warmest month's mean temperature on the chironomid fauna, we used general additive modelling (GAM; Hastie and Tibshirani, 1990; Szabó et al., 2020) and cross correlations with the CRU database, in which measured July and summer mean temperatures for the last 120 years were compared with PCA 1 axis scores and chironomid-inferred July and summer mean temperatures (Figures 3, 6 and 8, SM1 Supplemental Figure 6, SM1 Supplemental Table 2). This analysis shows a significant relationship between July and summer mean temperatures and sample scores of PC1. Since negative values along PC1 were associated with cold-tolerant (*H. marcidus*-type, July mean optimum: 13.5°C), wide tolerance (e.g. *Procladius*) and warm-indicator chironomid types (*Limnophyes-Paralimnophyes*) as well, PC1 negative values cannot be unequivocally connected to colder summer temperatures, they can be rather interpreted as reflecting deeper, mesotrophic lake conditions. Positive values along PC1, however, are associated with taxa predominantly indicating warmer summer temperatures (e.g. *Dicrotendipes notatus*-type, *Tanytarsus mendax*-type, July mean optimum: >16.5°C) and increasing macrophyte cover. Positive scores along PC1 can therefore be taken as representing the joint effect of warming and shallowing.

It is also important to note that *Prosilocerus* type N showed an increase in the chironomid record between ~1600 and 1900 CE. This taxon has affinity to eutrophic lakes (Brooks et al., 2007; Moller Pillot, 2013; Sæther and Wang, 1996; Wiederholm, 1983), but its July mean temperature tolerance and optimum are difficult to estimate. Since it is not present in the Swiss-Norwegian training set (Eggermont and Heiri, 2012; Heiri et al., 2011), and only occurs in low abundance (<1%) in the FPC training set (Luoto, 2009; Luoto et al., 2019; Płóciennik et al., 2021), its association with low July mean temperatures (13.3°C) remains uncertain. In addition, it was not detected in any of the Carpathian lake surface samples (Supplemental Material 2), therefore we know relatively little about the conditions that are optimal for the species represented by this type. Since it reached >10% between ~1600 and 1900 CE, it remains unresolved whether climate or trophic changes led to its proliferation in Lake Latoriței and chironomid-inferred July mean temperatures are also possibly biased by these factors.

#### Chironomid-based July mean temperature reconstruction: climatic trends in regional context

GAM, cross-correlation analyses and the above detailed taxonomical and training set weaknesses suggest that the chironomid fauna and its changes in Lake Latoriței can be used for quantitative July mean temperature reconstruction, but with limitations. These limitations, however, possibly also pertain to other biotic proxy-based reconstructions that have been used to determine climate and precipitation changes over the past 2000 years in Europe and worldwide (Jones et al., 1998; Mann, 2002; Mann et al., 2009; Pages 2k Consortium, 2013; Figure 1).

The goodness of the reconstruction is used to summarise the discrepancy between the observed values and the values expected. These are presented on Figure 6. Examining this, we can say that

the chironomid-based temperature reconstruction with the FPC training set seems statistically robust between ~750 and 1830 CE and less so before and after. Therefore, we restrict the discussion of the reconstructed temperature changes to this time interval.

Our chironomid based  $T_{July}$  reconstruction provided unbiased and statistically robust results from the final parts of the Late Antique Little Ice Age (LALIA), also called the Dark Ages. From ~750 CE the reconstruction is characterised by gradually increasing temperatures in both reconstructions that peak between ~1000 and 1200 CE (Figure 9). This is the Medieval Warm period (MWP: 900–1300 CE) that in north-western Europe was 0.6–1.2°C warmer than the 1880–1960 CE average (Christiansen and Ljungqvist, 2012; Lamb, 1965). Several reconstructions have been made for this period, but the extent of warming at the regional level is still unclear. There are also more and more multiproxy reconstructions underway in Europe from this period with heterogeneous results in different parts of Europe. In some cases, the proxy-records show no change compared to the reference period (Büntgen et al., 2006, 2011, 2016; Jones et al., 1998; Luterbacher et al., 2016; Mann et al., 2003, 2009; Pages 2k Consortium, 2013; Figure 9). On the other hand, continental summaries made by the Pages 2k Consortium (2013) show uniform warming in almost all continents, including Europe (Figure 9). If we look at the tree-ring-based reconstructions, summers in northern Europe were warmer (Büntgen et al., 2011), but in the Alps and Carpathians this period was characterised by alternating periods of warmer and colder temperatures (Büntgen et al., 2011, 2013, 2016; Popa and Kern, 2009). Chironomid-based  $T_{July}$  reconstructions from the Alps also indicate warming in this period (Larocque-Tobler et al., 2010, 2012; Millet et al., 2009), while similar studies in NW Europe suggest less stable warm July mean temperatures (Zawiska et al., 2017). The temperature reconstruction closest to our study area is tree-ring-based, and it comes from the Eastern Carpathians (Popa and Kern, 2009). This reconstruction does not cover the entire MWP (only 1100–1300 CE), but it suggests that this period was not uniformly warm in the Eastern Carpathians (Figure 9). Between 750 and 1350 CE our chironomid-based temperature reconstruction showed a more pronounced warming trend than the tree-ring-based reconstruction. Summers were stable and consistently relatively warm. In the reconstruction, the higher abundance of *Tanytarsus mendax*-type and the decrease of *M. insignilobus*-type are responsible for the inferred warming. Another tree-ring-based reconstruction from the West Carpathian Tatra Mts agrees with the findings of Popa and Kern (2009). According to this, warmer periods were only observed in the mid-11th century, during the 12th century and at the end of the 13th century (Büntgen et al., 2013). This difference by the different proxies is likely attributable to the different response time of the applied biological proxies. While tree-rings can reflect annual summer temperature change, chironomid assemblages from usually 1 cm thick layers represent several years, in some cases even over a decade. In addition, community change of chironomids takes place over several generations (Brooks et al., 2007; Corley and Massaferrò, 1998). Tree-ring based summer mean temperature reconstructions from the Austrian Alps show higher summer temperatures only in the early 10th century, the first half of the 11th century and the second half of the 12th century, with a maximum increase of 0.4°C relative to the reference period 1961–1990 (Figure 9; Büntgen et al., 2011, 2016). Chironomid-inferred  $T_{July}$  in the northern French Alps showed higher values between 680 and 1350 CE, which was connected to a significant glacier retreat in the northern Alps and a decrease in flooding of the Rhône (Millet et al., 2009). At Lake Anterne, the MWP is interrupted by a sharp decrease in reconstructed temperatures between ca. 1090 and 1160 CE. Holzhauser et al. (2005) report a simultaneous Great Aletsch glacier advance, while a summer temperature reconstruction by Büntgen et al. (2011) found a 1.5°C drop between 1020 and 1120 CE (Figure 9). This cooling event is not

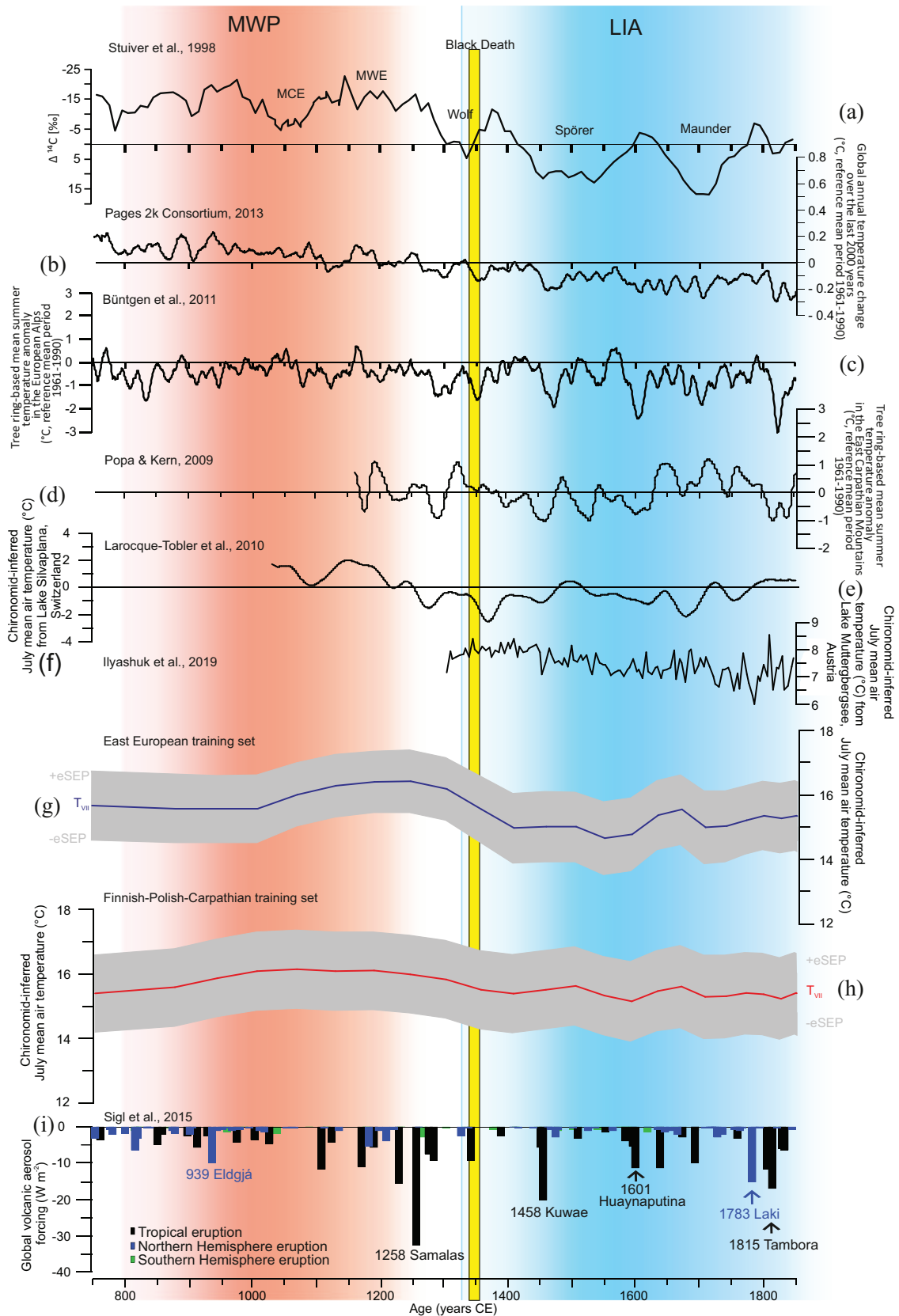


**Figure 9.** Loess-smoothed climate reconstructions for the period 750–1830 CE: (a) changes in in  $\Delta^{14}\text{C}$  solar activity (Stuiver et al., 1998); temperature changes based on global annual (b); Alps (c) and Eastern Carpathians (d) tree-ring-based summer temperature reconstructions (Büntgen et al., 2011; Pages 2k Consortium, 2013; Popa and Kern, 2009); two chironomid-based temperature reconstructions from the Alps ((e), Larocque-Tobler et al., 2010; (f), Ilyashuk et al., 2019); chironomid-based July mean temperature records for the last ~2000-year from Lake Latoritiei using the EE (g) and FPC (h) training sets; and (i) ice-core-derived global estimates of volcanic irradiance (GVF) (Sigl et al., 2015). Abbreviations: MWP: Mediaeval Warm Period; LIA: Little Ice Age; MCE: Medieval Cold Event; MWE: Medieval Warm Event.

indicated by our reconstruction. Another chironomid-based temperature reconstruction from the northern Swiss Alps, covering only the second half of this period (from 1100 CE), shows a 1.2°C increase in summer temperatures during the MWP (Larocque-Tobler et al., 2010, 2012).

In the statistically robust 750–1830 CE interval of the reconstruction marked coolings occurred between 1350 and 1600 CE (cooling rate maximum 1.1°C, average 0.7°C; Figure 9), followed by fluctuating summer temperatures between 1600 and 1830 CE (min. 14.7°C, max. 16.25 °C according to the FPC training set). This interval corresponds to the Little Ice Age (LIA). Cooling was connected to the higher abundance of *M. insignilobus*-type and *Prosilocerus* type N that are cold tolerant, and the latter also increased trophic level indicator (Brooks et al., 2007; Moller Pilot, 2013; Sæther and Wang, 1996; Wiederholm, 1983). Cooling indicated by the increasing abundance of these taxa in Lake Latoriței agrees well with the tree-ring-based temperature reconstruction of Popa and Kern (2009) in the Eastern Carpathians that shows cooler summers between 1370 and 1630 CE and 1820–1840 CE (Figure 9). Our results are in good agreement with the chironomid-based temperature reconstructions from the Alps that also identify this period (1370–1840 CE) as the main cooling phase of the LIA (Ilyashuk et al., 2019; Larocque-Tobler et al., 2010, 2012; Millet et al., 2009). From 1830 CE the increased human activity in the region significantly decreased the goodness of our reconstruction, therefore we do not discuss this part of the reconstruction.

## Conclusions

This study described climate changes reconstructed using sediments from a South Carpathian mountain lake, Lake Latoriței (1530 m a.s.l.) over the past 2000-year using chironomid-based warmest month mean temperature reconstruction and compared it with the results of other biotic and geochemical proxies. We used two different training sets, the Eastern-European (EE) and its extended version, the Finnish-Polish-Carpathian (FPC). When selecting the training sets, we considered the continentality of the area, as training sets developed for a given area, or similar climatic regions can best reflect smaller scale regional temperature change within the Holocene. Our results confirm this, FPC gave better results, especially between 800 and 1800 CE. Our results also suggest that during the Roman Warm Period (RWP; 180 BCE–810 CE) and Late Antique Little Ice Age (LALIA) intense streamflow, high erosional activity and high terrestrial organic matter input characterised the lake. The covariance of streamflow and erosional proxies with the chironomid community change suggested that our  $T_{July}$  reconstructions are biased in this period.

Between ~750 and ~1830 CE, the goodness-of-fit of the reconstruction improved significantly, covariance with environmental variables other than temperature decreased, and we considered this period as the most accurate part of the reconstruction. We detected a warmer period between ~750 and ~1360 CE corresponding with the Medieval Warm Period (MWP: 750–1360 CE). This was also detected in the Alps by chironomid-based July temperature reconstructions, where a uniform temperature increase was also observed in tree-ring-based summer temperature reconstructions. Our diatom record suggests that even though summers were likely significantly warmer, longer winters resulted in extended ice cover in the same period.

The Little Ice Age cooling started at ~1360 CE and peaked around 1600 and 1740 CE in our reconstructions, when we found a 0.7°C (EE) and 1.1°C (FPC) decrease in July mean air temperatures relative to the MWP warm peak around 1100 CE.

We conclude that despite the targeted training set building efforts of the last decades for the continental interior part of Europe (Korponai et al., n.d.; Luoto et al., 2019; Plóciennik et al., 2021), we still find some chironomid morphotypes poorly

represented in the training sets (e.g. *Prosilocerus*-type N). These taxa reduce the statistical power of the chironomid-inferred air temperature reconstructions. Nevertheless, we demonstrated that the mean July air temperature reconstruction based on the FPC training set shows very good agreement with other quantitative summer climate reconstructions from Eastern-Central Europe and the Alps.

## Author contributions

Zoltán Szabó: Investigation, Writing – original draft, Visualisation. Krisztina Buczkó: Investigation, Data curation, Writing – original draft, Writing - review & editing, Visualisation. János Korponai: Data curation, Visualisation, Investigation, Writing – review & editing. Tomi P. Luoto: Writing – review & editing. Róbert-Csaba Begy: Investigation, Visualisation. Aritina Haliuc: Visualisation, Investigation, Writing – original draft. Daniel Veres: Writing – review & editing. Ladislav Hamerlík: Writing – review & editing. Réka Csorba: Investigation, Visualisation. Andreea R. Zsigmond: Investigation, Writing – review & editing. Gabriella Darabos: Writing – review & editing. Nikolett Méhes: Investigation, data curation – review & editing. Csilla Kövér: sampling, investigation – review & editing. Enikő K. Magyari: Conceptualisation, Methodology, Supervision, Project administration, Funding acquisition, Writing – original draft, Writing – review & editing.

## Funding

The author(s) disclosed receipt of the following financial support for the research, authorship, and/or publication of this article: The research was supported by the European Union and the State of Hungary in the project of GINOP-2.3.2.-15-2016-00019 (Sustainable use of ecosystem services – research for mitigating the negative effect of climate change, land use change and biological invasion), co-financed by National Research Development and Innovation Office 2019-2.11-TÉT-2019-00034 (Chironomid based palaeoenvironmental and palaeoclimate reconstruction in the Carpathian region) and the National Multidisciplinary Laboratory for Climate Change (NKFIH-471-3/2021, RRF-2.3.1-21-2022-00014), the project NKFIH 129167, NKFIH 119208 and KKP 144209. Prepared with the Professional Support of the Doctoral Student Scholarship Program of the Co-Operative Doctoral Program of the Ministry of Innovation and Technology Financed from the National Research, Development And Innovation Fund. This work was also supported by a grant of the Romanian Ministry of Education and Research, CNCS-UEFISCDI, project number PN-III-P4-ID-PCE-2020-0914, within PNCDI III.

## ORCID iDs

Zoltán Szabó  <https://orcid.org/0000-0002-0899-2214>

Aritina Haliuc  <https://orcid.org/0000-0002-5681-8210>

## Data availability

The chironomid fossil data and the Finnish-Polish-Carpathian (FPC) training set used in this study is available in the following data publication: <https://data.mendeley.com/preview/scnz7xhcnx?a=1d4b8a3a-bc55-435e-b79a-57cbe73d4fab> Further data used in this study are available upon request.

## Supplemental material

Supplemental material for this article is available online.

## References

- Andersen T, Cranston P and Epler J (2013) Chironomidae of the Holarctic Region: Keys and diagnoses. Part 1 - Larvae. Available at: <https://www.abebooks.com/Chironomidae-Holarctic-Region-Keys-diagnoses-Part/30627041564/bd> (accessed 17 January 2023).

- Axford Y, Briner JP, Cooke CA et al. (2009) Recent changes in a remote Arctic lake are unique within the past 200,000 years. *Proceedings of the National Academy of Sciences of the United States of America* 106(44): 18443–18446.
- Battarbee RW and Charles DF (1986) Diatom-based pH reconstruction studies of acid lakes in Europe and North America: A synthesis. *Water, Air, and Soil Pollution* 30(1–2): 347–354.
- Bennett K (2007) Psimpoll 4.27. Available at: <http://chronos.qub.ac.uk/psimpoll/psimpoll.html> (accessed 17 January 2023).
- Bennett KD and Willis KJ (2001) Pollen. In: Smol JP, Birks HJB and Last WM (eds) *Tracking Environmental Change Using Lake Sediments. Volume 3: Terrestrial, Algal, And Siliceous Indicators*. Dordrecht, The Netherlands: Kluwer Academic Publishers, pp. 5–32.
- Bigler C, Heiri O, Krskova R et al. (2006) Distribution of diatoms, chironomids and cladocera in surface sediments of thirty mountain lakes in south-eastern Switzerland. *Aquatic Sciences* 68(2): 154–171.
- Bitušik P and Kubovčík V (1999) Sub-fossil chironomids (Diptera: Chironomidae) from the sediments of the Nižné Terianske pleso (High Tatra Mts., Slovakia). *Dipterologica Bohemoslovaca* 9: 11–20.
- Blaauw M (2010) R-Code for ‘classical’ age-modelling (CLAM V1.0) of radiocarbon sequences. Available at: <https://doi.pangaea.de/10.1594/PANGAEA.873023> (accessed 17 January 2023).
- Brisset E, Guitier F, Miramont C et al. (2017) The overlooked human influence in historic and prehistoric floods in the European Alps. *Geology* 45: 347–350.
- Brodersen K and Anderson N (2002) Distribution of chironomids (Diptera) in low arctic West Greenland lakes: Trophic conditions, temperature and environmental reconstruction. *Freshwater Biology* 47(6): 1137–1157.
- Brodersen KP and Quinlan R (2006) Midge as palaeoindicators of lake productivity, eutrophication and hypolimnetic oxygen. *Quaternary Science Reviews* 25(15–16): 1995–2012.
- Brooks SJ, Langdon PG and Heiri O (2007) *The Identification and Use of Palaearctic Chironomidae Larvae in Palaeoecology Technical Guide No (10)*. London: Quaternary Research Association (Great Britain), p.276.
- Büntgen U, Frank DC, Nievergelt D et al. (2006) Summer temperature variations in the European Alps, A.D. 755–2004. *Journal of Climate* 19(21): 5606–5623.
- Büntgen U, Kyncl T, Ginzler C et al. (2013) Filling the Eastern European gap in millennium-long temperature reconstructions. *Proceedings of the National Academy of Sciences of the United States of America* 110(5): 1773–1778.
- Büntgen U, Myglan VS, Ljungqvist FC et al. (2016) Cooling and societal change during the Late Antique Little Ice Age from 536 to around 660 AD. *Nature Geoscience* 9(3): 231–236.
- Büntgen U, Tegel W, Nicolussi K et al. (2011) 2500 years of European climate variability and human susceptibility. *Science* 331(6017): 578–582.
- Bledzki LA and Rybak JI (2016) *Freshwater Crustacean Zooplankton of Europe*. Cham: Springer International Publishing.
- Cantonati M, Zorza R, Bertoli M et al. (2021) Recent and subfossil diatom assemblages as indicators of environmental change (including fish introduction) in a high-mountain lake. *Ecological Indicators* 125: 107603.
- Christiansen B and Ljungqvist FC (2012) The extra-tropical Northern Hemisphere temperature in the last two millennia: Reconstructions of low-frequency variability. *Climate of the Past* 8(2): 765–786.
- Corley J and Massafiero J (1998) Long term turnover of a fossil community of chironomids (Diptera) from Lake Mascardi (Patagonia, Argentina). *Journal of the Kansas Entomological Society* 71(4): 407–413.
- Diaconu A, Tan I, Knorr K et al. (2020) A multi-proxy analysis of hydroclimate trends in an ombrotrophic bog over the last millennium in the Eastern Carpathians of Romania. *Palaeogeography, Palaeoclimatology, Palaeoecology* 538: 109390.
- Eddy JA (1977) Climate and the changing sun. *Climatic Change* 1(2): 173–190.
- Eggermont H and Heiri O (2012) The chironomid-temperature relationship: Expression in nature and palaeoenvironmental implications. *Biological Reviews* 87(2): 430–456.
- Engels S, Bohncke SJP, Heiri O et al. (2008) Intraregional variability in chironomid-inferred temperature estimates and the influence of river inundations on lacustrine chironomid assemblages. *Journal of Paleolimnology* 40: 129–142.
- Engels S, Self AE, Luoto TP et al. (2014) A comparison of three Eurasian chironomid–climate calibration datasets on a W–E continentality gradient and the implications for quantitative temperature reconstructions. *Journal of Paleolimnology* 51(4): 529–547.
- Feurdean A, Florescu G, Vannière B et al. (2017) Fire has been an important driver of forest dynamics in the Carpathian Mountains during the Holocene. *Forest Ecology and Management* 389: 15–26.
- Feurdean A, Galka M, Kuske E et al. (2015) Last Millennium hydro-climate variability in Central–Eastern Europe (Northern Carpathians, Romania). *Holocene* 25(7): 1179–1192.
- Feurdean A, Galka M, Tanțău I et al. (2016) Tree and timberline shifts in the northern Romanian Carpathians during the Holocene and the responses to environmental changes. *Quaternary Science Reviews* 134: 100–113.
- Gandouin E, Maasri A, Van Vliet-Lanoë B et al. (2006) Chironomid (Insecta: Diptera) assemblages from a gradient of lotic and lentic waterbodies in river floodplains of France: A methodological tool for paleoecological applications. *Journal of Paleolimnology* 35: 149–166.
- Gannon JE (1971) Two counting cells for the enumeration of zooplankton micro-Crustacea. *Transactions of the American Microscopical Society* 90(4): 486.
- Gheorghiu DM, Hosu M, Corpade C et al. (2015) Deglaciation constraints in the Parâng Mountains, southern Romania, using surface exposure dating. *Quaternary International* 388: 156–167.
- Giaime M, Magne G, Bivolaru A et al. (2019) Halmyris: Geoarchaeology of a fluvial harbour on the Danube Delta (Dobrogea, Romania). *Holocene* 29(2): 313–327.
- Grimm EC and Jacobson G (1992) Fossil-pollen evidence for abrupt climate changes during the past 18 000 years in eastern North America. *Climate Dynamics* 6(3–4): 179–184.
- Guiry MD and Guiry GM (2023) AlgaeBase. World-wide electronic publication. National University of Ireland, Galway. Available at: <https://www.algaebase.org>
- Halecki O (1950) *The Limits and Divisions on European History*. New York: Sheed & Ward, p.120.
- Haliuc A, Buczkó K, Hutchinson SM et al. (2020) Climate and land-use as the main drivers of recent environmental change in a mid-altitude mountain lake, Romanian Carpathians. *PLoS ONE* 15: 1–30.
- Haliuc A, Veres D, Brauer A et al. (2017) Palaeohydrological changes during the mid and Late Holocene in the Carpathian area, central-eastern Europe. *Global and Planetary Change* 152: 99–114.
- Hamerlík L and Bitušik P (2009) The distribution of littoral chironomids along an altitudinal gradient in High Tatra Mountain lakes: Could they be used as indicators of climate change? *Annales de Limnologie* 45(3): 145–156.
- Hamerlík L, Dobriková D, Szarłowicz K et al. (2016) Lake biota response to human impact and local climate during the last 200 years: A multi-proxy study of a subalpine lake (Tatra Mountains, W Carpathians). *Science of the Total Environment* 545–546: 320–328.

- Harris I, Jones PD, Osborn TJ et al. (2014) Updated high-resolution grids of monthly climatic observations – The CRU TS3.10 Dataset. *International Journal of Climatology* 34(3): 623–642.
- Hastie TJ and Tibshirani RJ (1990) *Generalized Additive Models*. London: Chapman & Hall.
- Heiri O, Brooks SJ, Birks HJB et al. (2011) A 274-lake calibration data-set and inference model for chironomid-based summer air temperature reconstruction in Europe. *Quaternary Science Reviews* 30(23–24): 3445–3456.
- Heiri O and Lotter AF (2001) Effect of low count sums on quantitative environmental reconstructions: An example using subfossil chironomids. *Journal of Paleolimnology* 26: 343–350.
- Holzhauser H, Magny M and Zumbühl HJ (2005) Glacier and lake-level variations in west-central Europe over the last 3500 years. *Holocene* 15(6): 789–801.
- Hořická Z, Stuchlík E, Hudec I et al. (2006) Acidification and the structure of crustacean zooplankton in mountain lakes: The Tatra Mountains (Slovakia, Poland). *Biologia* 61(S18): S121–S134.
- Hubay K, Braun M, Buczkó K et al. (2018) Holocene environmental changes as recorded in the geochemistry of glacial lake sediments from Retezat Mountains, South Carpathians. *Quaternary International* 477: 19–39.
- Ilyashuk EA, Heiri O, Ilyashuk BP et al. (2019) The Little Ice Age signature in a 700-year high-resolution chironomid record of summer temperatures in the Central Eastern alps. *Climate Dynamics* 52(11): 6953–6967.
- Jones PD, Briffa KR, Barnett TP et al. (1998) High-resolution palaeoclimatic records for the last millennium: interpretation, integration and comparison with General Circulation model control-run temperatures. *Holocene* 8(4): 455–471.
- Juggins S (2007) *C2 Version 1.5 User Guide. Software for Ecological and Palaeoecological Data Analysis and Visualisation*. Newcastle upon Tyne: Newcastle University. Available at: <https://www.staff.ncl.ac.uk/stephen.juggins/software/code/C2.pdf>
- Juggins S (2017) rioja: Analysis of Quaternary Science Data, R package version (0.9-21). Available at: <http://cran.r-project.org/package=rioja>.
- Keller B, Burgi HR, Sturm M et al. (2002) Ehippia and Daphnia abundances under changing trophic conditions. *Verhandlungen: Internationale Vereinigung für Theoretische und Angewandte Limnologie* 28: 851–855.
- Korponai J, Kövér C, Méhes N et al. (n.d.) How do sediment surface diatom, cladoceran and chironomid taphocoenoses of temperate mountain lakes reflect the environmental variability? An insight from the South Carpathian Mts. In *press in Water (MDPI)*.
- Korponai J, Varga KA, Lengré T et al. (2011) Paleolimnological reconstruction of the trophic state in Lake Balaton (Hungary) using Cladocera remains. *Hydrobiologia* 676(1): 237–248.
- Krammer K and Lange-Bertalot H (1986) Bacillariophyceae. 1. Teil: Naviculaceae. In: Ettl H, Gerloff J, Heynig H et al. (eds) *Süßwasserflora von Mitteleuropa, Band 1/2*. Jena, Germany: Gustav Fisher Verlag, pp. 1–876.
- Krammer K and Lange-Bertalot H (1988) Bacillariophyceae. 2. Teil: Bacillariaceae, Epithemiaceae, Surirellaceae. In: Ettl H, Gerloff J, Heynig H et al. (eds) *Süßwasserflora von Mitteleuropa, Band 2/2*. Jena, Germany: Gustav Fisher Verlag, pp. 1–610.
- Krammer K and Lange-Bertalot H (1991a) Bacillariophyceae. 3. Teil: Centrales, Fragilariaceae, Eunotiaceae. In: Ettl H, Gerloff J, Heynig H et al. (eds) *Süßwasserflora von Mitteleuropa, Band 2/3*. Stuttgart, Germany: Gustav Fisher Verlag, pp. 1–576.
- Krammer K and Lange-Bertalot H (1991b) Bacillariophyceae. 4. Teil: Achnantheaceae. *Kritische Ergänzungen zu Navicula (Lineolatae) und Gomphonema*. In: Ettl H, Gartner G, Gerloff J et al. (eds) *Süßwasserflora von Mitteleuropa, Band 2/4*. Stuttgart, Germany: Gustav Fisher Verlag, pp. 1–437.
- Kuefner W, Hofmann A, Ossyssek S et al. (2020) Composition of highly diverse diatom community shifts as response to climate change: A down-core study of 23 central European mountain lakes. *Ecological Indicators* 117: 106590.
- Lamb H (1965) The early medieval warm epoch and its sequel. *Palaeogeography Palaeoclimatology Palaeoecology* 1(C): 13–37.
- Langdon P, Ruiz Z, Brodersen K et al. (2006) Assessing lake eutrophication using chironomids: Understanding the nature of community response in different lake types. *Freshwater Biology* 51(3): 562–577.
- Lange-Bertalot H, Hofmann G, Werum M et al. (2017) *Freshwater Benthic Diatoms of Central Europe: Over 800 Common Species Used in Ecological Assessment. English Edition with Updated Taxonomy and Added Species*. Koeltz Botanical Books, Schmitten-Oberreifenberg.
- Lange-Bertalot H and Metzeltin D (1996) Indicators of oligotrophy – 800 taxa representative of three ecologically distinct lake types, carbonate buffered – Oligodystrophic – Weakly buffered soft water. In: Lange-Bertalot H (ed.) *Iconographia Diatomologica. Annotated Diatom Micrographs*, vol. 2, Ecology, Diversity, Taxonomy. Königstein, Germany: Koeltz Scientific Books, p. 390.
- Larocque I and Bigler C (2004) Similarities and discrepancies between chironomid- and diatom-inferred temperature reconstructions through the Holocene at Lake 850, northern Sweden. *Quaternary International* 122(1): 109–121.
- Larocque I, Grosjean M, Heiri O et al. (2009) Comparison between chironomid-inferred July temperatures and meteorological data AD 1850–2001 from varved Lake Silvaplana, Switzerland. *Journal of Paleolimnology* 41(2): 329–342.
- Larocque-Tobler I, Grosjean M, Heiri O et al. (2010) Thousand years of climate change reconstructed from chironomid subfossils preserved in varved lake Silvaplana, Engadine, Switzerland. *Quaternary Science Reviews* 29(15–16): 1940–1949.
- Larocque-Tobler I, Stewart MM, Quinlan R et al. (2012) A last millennium temperature reconstruction using chironomids preserved in sediments of anoxic seebergsee (Switzerland): Consensus at local, regional and Central European scales. *Quaternary Science Reviews* 41: 49–56.
- Legendre P and Gallagher E (2001) Ecologically meaningful transformations for ordination of species data. *Oecologia* 129(2): 271–280.
- Legendre P and Legendre L (2012) Numerical ecology Ch 6 - multidimensional qualitative data. *Developments in Environmental Modelling* 24: 337–424.
- Longman J, Veres D, Ersek V et al. (2019) Runoff events and related rainfall variability in the Southern Carpathians during the last 2000 years. *Scientific Reports* 9: 1–14.
- Lotter AF and Bigler C (2000) Do diatoms in the Swiss Alps reflect the length of ice-cover? *Aquatic Sciences* 62(2): 125–141.
- Luoto T, Kotrys B and Plóciennik M (2019) East European chironomid-based calibration model for past summer temperature reconstructions. *Climate Research* 77: 63–76.
- Luoto TP (2009) Subfossil Chironomidae (Insecta: Diptera) along a latitudinal gradient in Finland: Development of a new temperature inference model. *Journal of Quaternary Science* 24(2): 150–158.
- Luoto TP (2010) Hydrological change in lakes inferred from midge assemblages through use of an intralake calibration set. *Ecological Monographs* 80(2): 303–329.



- Luoto TP, Helama S and Nevalainen L (2013) Stream flow intensity of the Saavanjoki River, eastern Finland, during the past 1500 years reflected by mayfly and caddisfly mandibles in adjacent lake sediments. *Journal of Hydrology* 476: 147–153.
- Luoto TP and Nevalainen L (2012) Ecological responses of aquatic invertebrates to climate change over the past ~400 years in a climatically ultra-sensitive lake in the Niedere Tauern alps (Austria). *Fundamental and Applied Limnology: Official Journal of the International Association of Theoretical and Applied Limnology* 181(3): 169–181.
- Luoto TP, Nevalainen L, Kultti S et al. (2011) An evaluation of the influence of water depth and river inflow on quantitative Cladocera-based temperature and lake level inferences in a shallow boreal lake. *Hydrobiologia* 676(1): 143–154.
- Luterbacher J, Werner JP, Smerdon JE et al. (2016) European summer temperatures since Roman times. *Environmental Research Letters* 11(2): 024001.
- Mann M, Amman C, Bradley R et al. (2003) On past temperatures and anomalous late-20th-century warmth. *Eos* 84(27): 256–256.
- Mann ME (2002) Medieval climatic optimum. In: MacCracken MC and Perry JS (eds) *Encyclopedia of Global Environmental Change*, vol. 1. Chichester: John Wiley & Sons, Ltd, pp.514–516.
- Mann ME, Zhang Z, Rutherford S et al. (2009) Global signatures and dynamical origins of the Little Ice Age and medieval climate anomaly. *Science* 326: 1256–1260.
- Marinescu E, Marinescu IE, Vladut A et al. (2013) Forest cover change in the Parâng-Cindrel Mountains of the Southern Carpathians, Romania. In: Kozak J, Ostapowicz K, Bytnerowicz A et al. (eds) *The Carpathians: Integrating Nature and Society Towards Sustainability, Environmental Science and Engineering*. Berlin, Heidelberg: Springer.
- McKeown M and Potito A (2015) Assessing recent climatic and human influences on chironomid communities from two moderately impacted lakes in western Ireland. *Hydrobiologia* 765(1): 245–263.
- Medeiros AS, Gajewski K, Porinchu DF et al. (2015) Detecting the influence of secondary environmental gradients on chironomid-inferred paleotemperature reconstructions in northern North America. *Quaternary Science Reviews* 124: 265–274.
- Michailova P (2009) Karyotype and external morphology of *Dicrotendipes lobiger* Kieffer, 1921 (Diptera: Chironomidae) from some regions in Bulgaria. *Acta Zoologica. Bulgarica* 61(2): 115–121.
- Micu DM, Dumitrescu A, Cheval S et al. (2015) *Climate of the Romanian Carpathians*. Cham: Springer, pp.73–148.
- Millet L, Arnaud F, Heiri O et al. (2009) Late-Holocene summer temperature reconstruction from chironomid assemblages of Lake Anterne, northern French alps. *Holocene* 19(2): 317–328.
- Moller Pillot HKM (2013) *Chironomidae Larvae. Vol 3: Aquatic Orthoclaadiinae*. Zeist: KNNV.
- Moore PD, Webb JA and Collinson ME (1991) *Pollen Analysis*. Chichester: Wiley-Blackwell Publishing.
- Newell RL and Baumann RW (2013) Studies on distribution and diversity of Nearshore Ephemeroptera and Plecoptera in selected lakes of Glacier National Park, Montana. *Western North American Naturalist* 73: 230–236.
- Oksanen JF, Guillaume Blanchet R, Legendre P et al. (2015) Package ‘vegan’. *R package version 2.3-4*.
- Pages 2k Consortium (2013) Continental-scale temperature variability during the past two millennia. *Nature Geoscience* 6(5): 339–346.
- Pinczés Z (1995) Déli-felföld természeti földrajza (Natural geography of the Southern Highlands). *Jegyzet (Note), KLTE, Debrecen*: 149.
- Popa I and Kern Z (2009) Long-term summer temperature reconstruction inferred from tree-ring records from the Eastern Carpathians. *Climate Dynamics* 32: 1107–1117.
- Pörtner H, Roberts D, Tignor M et al. (2022) IPCC, 2022: Climate Change 2022: Impacts, Adaptation and Vulnerability. Contribution of Working Group II to the Sixth Assessment Report of the Intergovernmental Panel on Climate Change. Cambridge, UK and New York, NY: Cambridge University Press.; 3056. DOI: 10.1017/9781009325844.
- Potito AP, Woodward CA, McKeown M et al. (2014) Modern influences on chironomid distribution in western Ireland: potential for palaeoenvironmental reconstruction. *Journal of Paleolimnology* 52(4): 385–404.
- Plóciennik M, Jakiel A and Forsytek J (2021) Multi-proxy inferred hydroclimatic conditions at Bęczkowice fen (central Poland); the influence of fluvial processes and human activity in the stone age. *Acta Geographica Lodziana* 111: 135–157.
- R Core Team (2020) *R: A Language and Environment for Statistical Computing*. Vienna: R Foundation for Statistical Computing. Available at: <http://www.r-project.org/index.html> (accessed 17 January 2023).
- Reavie ED and Kireta AR (2015) Centric, araphid and eunotioid diatoms of the coastal Laurentian great lakes. *Bibliotheca Diatomologica* 62: 1–184.
- Reille M (1992) *Pollen et spores d'Europe et d'Afrique du Nord*. Marseille, France: Laboratoire de Botanique Historique et Palynologie.
- Reille M (1995) *Pollen et spores d'Europe et d'Afrique du Nord, Supplement 1*. Marseille, France: Laboratoire de Botanique Historique et Palynologie.
- Reille M (1998) *Pollen et spores d'Europe et d'Afrique du Nord, Supplement 2*. Marseille, France: Laboratoire de Botanique Historique et Palynologie.
- Reimer PJ, Austin WEN, Bard E et al. (2020) The IntCal20 Northern Hemisphere radiocarbon age calibration curve (0–55 cal kBP). *Radiocarbon* 62(4): 725–757.
- Rieradevall M and Brooks SJ (2001) An identification guide to subfossil Tanytopodinae larvae (Insecta: Diptera: Chironomidae) based on cephalic setation. *Journal of Paleolimnology* 25(1): 81–99.
- Sacherová V, Kršková R, Stuchlík E et al. (2006) Long-term change of the littoral Cladocera in the Tatra Mountain lakes through a major acidification event. *Biologia* 61(S18): S109–S119.
- Sæther OA and Wang X (1996) Revision of the orthoclad genus *Prosilocerus* Kieffer (= *Tokunagayusurika* Sasa) (Diptera: Chironomidae). *Entomologia Scandinavica* 27(4): 441–479.
- Sebestyén O (1965) Kládocera tanulmányok a Balatonon - III. Történelmi előtanulmányok – Cladocera studies in Lake Balaton - III. Preliminary studies for lake history investigations. *Annales Instituti Biologici (Tihany)* 32: 229–256.
- Self AE, Brooks SJ, Birks HJB et al. (2011) The distribution and abundance of chironomids in high-latitude Eurasian lakes with respect to temperature and continentality: Development and application of new chironomid-based climate-inference models in northern Russia. *Quaternary Science Reviews* 30(9–10): 1122–1141.
- Sigl M, Winstrup M, McConnell JR et al. (2015) Timing and climate forcing of volcanic eruptions for the past 2,500 years. *Nature* 523(7562): 543–549.
- Smol JP (2019) Under the radar: Long-term perspectives on ecological changes in lakes. *Proceedings of The Royal Society B Biological Sciences* 286(1906): 20190834.
- Solem J and Birks HH (2000) Late-glacial and early-Holocene Trichoptera (Insecta) from Krakenes Lake, western Norway. *Journal of Paleolimnology* 23: 49–56.

- Spinoni J, Vogt J and Barbosa P (2015) European degree-day climatologies and trends for the period 1951–2011. *International Journal of Climatology* 35(1): 25–36.
- Stuchlík E, Bitušík P, Hardekopf DW et al. (2017) Complexity in the biological recovery of Tatra Mountain Lakes from acidification. *Water Air & Soil Pollution* 228(5): 184.
- Stuiver M and Reimer PJ (1993) Extended 14C data base and revised CALIB 3.0 14C Age Calibration Program. *Radiocarbon* 35(1): 215–230.
- Stuiver M, Reimer PJ and Braziunas TF (1998) High-precision radiocarbon age calibration for terrestrial and marine samples. *Radiocarbon* 40(3): 1127–1151.
- Szabó Z, Buczkó K, Haliuc A et al. (2020) Ecosystem shift of a mountain lake under climate and human pressure: A move out from the safe operating space. *Science of the Total Environment* 743: 140584–140617.
- Szeroczyńska K and Sarmaja-Korjonen K (2007) *Atlas of Subfossil Cladocera From Central and Northern Europe*. Świecie: Friends of Lower Vistula Society, pp.1–84.
- Taylor KJ, Potito AP, Beilman DW et al. (2013) Palaeolimnological impacts of early prehistoric farming at Lough Dargan, County Sligo, Ireland. *Journal of Archaeological Science* 40(8): 3212–3221.
- Ter Braak C and Juggins S (1993) Weighted averaging partial least squares regression (WA-PLS): An improved method for reconstructing environmental variables from species assemblages. *Hydrobiologia* 269–270(1): 485–502.
- Tóth M, Buczkó K, Specziár A et al. (2018) Limnological changes in South Carpathian glacier-formed lakes ( Retezat Mountains, Romania) during the late glacial and the holocene: A synthesis. *Quaternary International* 477: 138–152.
- Tóth M, Magyari EK, Buczkó K et al. (2015) Chironomid-inferred Holocene temperature changes in the South Carpathians (Romania). *Holocene* 25(4): 569–582.
- Tóth M, van Hardenbroek M, Bleicher N et al. (2019) Pronounced early human impact on lakeshore environments documented by aquatic invertebrate remains in waterlogged Neolithic settlement deposits. *Quaternary Science Reviews* 205: 126–142.
- Tremel B, Frey S, Yan N et al. (2000) Habitat specificity of littoral Chydoridae (Crustacea, Branchiopoda, Anomopoda) in Plastic Lake, Ontario, Canada. *Hydrobiologia* 432(1981): 195–205.
- Urdea P and Florin V (2000) Aspect of periglacial relief in the Parâng Mountains. *Revista de Geomorfologie* 2: 35–59.
- Urdea P, Onaca A, Ardelean F et al. (2011) New evidence on the Quaternary glaciation in the Romanian Carpathians. *Developments in Quaternary Science* 15(4): 305–322.
- Vallenduuk H and Moller Pillot HKM (2009) *Chironomidae Larvae. Vol 2: Biology and Ecology of the Chironomini*. Utrecht: KNNV.
- Vallenduuk HJ and Moller Pillot HKM (2007) *Chironomidae Larvae. Vol 1: General Ecology and Tanypodinae*. Utrecht: KNNV.
- Velle G, Brooks SJ, Birks HJB et al. (2005) Chironomids as a tool for inferring holocene climate: An assessment based on six sites in southern Scandinavia. *Quaternary Science Reviews* 24(12–13): 1429–1462.
- Vijverberg J and Boersma M (1997) Long-term dynamics of small-bodied and large-bodied cladocerans during the eutrophication of a shallow reservoir, with special attention for *Chydorus sphaericus*. *Hydrobiologia* 360: 233–242.
- Vincze I, Orbán I, Birks HH et al. (2017) Holocene treeline and timberline changes in the South Carpathians (Romania): Climatic and anthropogenic drivers on the southern slopes of the Retezat Mountains. *Holocene* 27(11): 1613–1630.
- Voiculescu M and Török-Oance M (2000) The analysis of the snow layer in the context of global climate change in the Southern Carpathians (Romanian Carpathians.). Available at: [https://www.academia.edu/14473826/THE\\_ANALYSIS\\_OF\\_THE\\_SNOW\\_LAYER\\_IN\\_THE\\_CONTEXT\\_OF\\_GLOBAL\\_CLIMATE\\_CHANGE\\_IN\\_THE\\_SOUTHERN\\_CARPATHIANS\\_ROMANIAN\\_CARPATHIANS](https://www.academia.edu/14473826/THE_ANALYSIS_OF_THE_SNOW_LAYER_IN_THE_CONTEXT_OF_GLOBAL_CLIMATE_CHANGE_IN_THE_SOUTHERN_CARPATHIANS_ROMANIAN_CARPATHIANS)
- Vondrák D, Schafstall NB, Chvojka P et al. (2019) Postglacial succession of caddisfly (Trichoptera) assemblages in a central European montane lake. *Biologia* 74: 1325–1338.
- Walker IR (1987) Chironomidae (Diptera) in paleoecology. *Quaternary Science Reviews* 6(1): 29–40.
- Walker IR (2001) Midges: Chironomidae and related Diptera. In: Smol JP, Birks HJB and Last WM (eds) *Tracking Environmental Change Using Lake Sediments*, vol. 4. Dordrecht: Springer Netherlands, pp.43–66.
- Wiederholm T (1983) Chironomidae of the Holarctic region. Keys and diagnoses. Part 1: Larvae. *Entomologica scandinavica* 19: 573.
- Wilson S and Gajewski K (2004) Modern Chironomid assemblages and their relationship to physical and chemical variables in southwest Yukon and northern British Columbia Lakes modern Chironomid assemblages and their relationship to physical and chemical variables in southwest Yukon and northern British Columbia Lakes. *Arctic, Antarctic, and Alpine Research* 36(4): 446–455.
- Zawiska I, Luoto TP, Nevalainen L et al. (2017) Climate variability and lake ecosystem responses in western Scandinavia (Norway) during the last Millennium. *Palaeogeography Palaeoclimatology Palaeoecology* 466: 231–239.
- Zheng T, Cao Y, Peng J et al. (2020) Effects of climate warming and nitrogen deposition on subtropical montane ponds (central China) over the last two centuries: Evidence from subfossil chironomids. *Environmental Pollution* 262: 114256.